molecular pharmaceutics

Article

pubs.acs.org/molecularpharmaceutics

Bubble Liposomes and Ultrasound Promoted Endosomal Escape of TAT-PEG Liposomes as Gene Delivery Carriers

Daiki Omata,[†] Yoichi Negishi,*[,†] Shoko Hagiwara,[†] Sho Yamamura,[†] Yoko Endo-Takahashi,[†] Ryo Suzuki,[‡] Kazuo Maruyama,[‡] Motoyoshi Nomizu,[§] and Yukihiko Aramaki[†]

[†]Department of Drug Delivery and Molecular Biopharmaceutics, School of Pharmacy, Tokyo University of Pharmacy and Life Sciences, Hachioji, Tokyo 192-0392, Japan

[‡]Department of Biopharmaceutics, School of Pharmaceutical Sciences, Teikyo University, Sagamihara, Kanagawa 252-5195, Japan

[§]Department of Clinical Biochemistry, School of Pharmacy, Tokyo University of Pharmacy and Life Sciences, Hachioji, Tokyo 192-0392, Japan

ABSTRACT: We have previously developed laminin-derived AG73 peptide-labeled poly(ethylene glycol)-modified liposomes (AG73-PEG liposomes) for selective cancer gene therapy and reported that Bubble liposomes (BLs) and ultrasound (US) exposure could accelerate the endosomal escape of AG73-PEG liposomes, leading to the enhancement of transfection efficiency; however, it is still unclear whether BLs and US exposure can also enhance the transfection efficiency of other vectors. We therefore assessed the effect of BLs and US exposure on the gene transfection efficiency of *trans*-activating transcriptor (TAT) peptide modified PEG liposomes. Although TAT-PEG liposomes were efficiently internalized into cells, the efficacy of endosomal escape was insufficient. The transfection efficiencies of TAT-PEG liposomes were enhanced by about 30-fold when BLs and US exposure were used. We also confirmed that BLs and US exposure could not enhance the direct transportation of TAT-PEG liposomes into cells. Confocal microscopy showed that BLs and US exposure promoted endosomal escape of TAT-PEG liposomes. Our results suggested that BLs and US exposure could enhance transfection efficiency by promoting endosomal escape, which was independent of modified molecules of carriers. Thus, BLs and US exposure can be a useful tool to achieve efficient gene transfection by improving endosomal escape of various carriers.

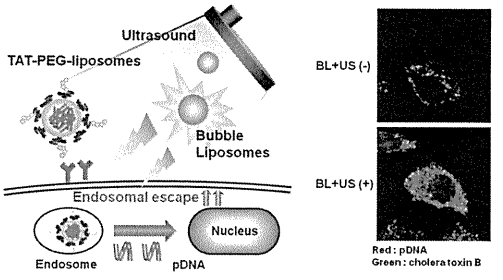

KEYWORDS: *Bubble liposomes, gene delivery, TAT peptide, ultrasound*

INTRODUCTION

Successful gene therapy depends on the efficient and safe delivery of genes into the desired tissues and cells. It is therefore necessary to develop efficient delivery vectors or methods for gene therapy. Nonviral vectors, such as cationic lipids or polymers, continue to be an attractive alternative to viral vectors due to their safety and convenient large-scale production, but their relatively low transfection efficiency compared with viral vectors is a major disadvantage.[1] In nonviral gene therapy, high transfection activity is required to improve the rate-limiting steps such as cellular internalization, endosomal escape, nuclear transfer, and intranuclear transcription.[2,3] In these steps, endosomal escape is considered one of the most important steps. When the vector cannot overcome this process, the cargo is degraded in lysosomes, leading to decreased gene transfection efficiency. For efficient endosomal escape, some studies have developed carriers equipped with functions such as pH sensitivity,[4,5] temperature dependence,[6] or photosensitivity.[7]

We have previously developed laminin-derived AG73 peptide-labeled poly(ethylene glycol) modified liposomes (AG73-PEG liposomes) for selective cancer gene therapy.[8] We also reported that echo-contrast gas-entrapping PEG liposomes, called "Bubble liposomes" (BLs), and ultrasound (US) exposure could accelerate the endosomal escape of AG73-PEG liposomes, leading to enhanced transfection efficiency.[9] It is expected that BLs and US exposure may promote the endosomal escape of various carriers and enhance their transfection efficiency; however, it is still unclear whether BLs and US exposure can enhance the transfection efficiency of vectors other than AG73-PEG liposomes, and the effect of BLs and US exposure on the transfection efficiency and endosomal escape of other functional molecule modified gene delivery carriers is not clearly understood.

Cell-penetrating peptides (CPPs), such as TAT and R8 peptides, are able to facilitate penetration through cell membranes and translocate different cargo into cells.[10] The TAT peptide, derived from a human immunodeficiency virus trans-acting transcriptional activator, has been studied to achieve highly efficient gene delivery and to develop TAT-modified liposomes and a polyplex.[11,12] The majority of these carriers were internalized via endocytosis and were required to achieve endosomal escape for efficient gene transfection.[13] Additionally, TAT-modified carriers equipped with components enhancing endosomal escape have been developed.[14]

Received: July 13, 2011
Revised: October 6, 2011
Accepted: October 24, 2011
Published: October 24, 2011

We therefore prepared TAT-modified liposomes as a model to evaluate the effect of BLs and US exposure on gene transfection efficiency via endosomal escape.

In this study, to assess the utility of BLs and US exposure for efficient gene delivery in general, we focused on TAT peptide and evaluated the effect of BLs and US exposure on the gene transfection efficiency of TAT-modified liposomes.

EXPERIMENTAL SECTION

Materials. The plasmid pCMV-Luc is an expression vector encoding the firefly luciferase gene under the control of cytomegalovirus promoter. Fluorescein isothiocyanate-conjugated cholera toxin B subunit (FITC-CTB), chloroquine, chlorpromazine and protamine were purchased from Sigma (St. Louis, MO). Cy3-labeled pDNA was purchased from Mirus Bio, LLC (Madison, WI). Genistein was purchased from Wako Pure Chemical Industries, Ltd. (Osaka, Japan). Amiloride was purchased from Calbiochem (San Diego, CA).

Cell Lines and Cultures. HeLa cells (human cervical cell line) were cultured in Dulbecco's modified Eagle's medium (DMEM; Kohjin Bio Co. Ltd., Tokyo, Japan), supplemented with 10% fetal bovine serum (FBS; Equitech Bio Inc., Kerrville, TX), penicillin (100 U/mL), and streptomycin (100 μg/mL) at 37 °C in a humidified 5% CO_2 atmosphere.

Preparation of TAT-PEG Liposomes. The Cys-TAT peptide (CGG-GRKKRRQRRRPPQ) was synthesized manually using the 9-fluorenylmethoxycarbonyl (Fmoc)-based solid-phase strategy, prepared in the COOH-terminal amide form and purified by reverse-phase high performance liquid chromatography. Liposomes were prepared by the hydration method. pDNA diluted in 10 mM HEPES buffer (pH 7.4) was condensed using protamine (N/P = 5.0). The complex of pDNA and protamine was added to a lipid film composed of 1,2-dioleoyl-*sn*-glycero-3-phospho-*rac*-1-glycerol (DOPG) (AVANTI Polar Lipids Inc., Alabaster, AL), 1,2-dioleoyl-*sn*-glycero-3-phosphoethanolamine (DOPE) (AVANTI Polar Lipids, Inc.), and 1,2-distearoyl-*sn*-glycero-3-phophatidylethanolamine-polyethyleneglycol-maleimide (DSPE-PEG_{2000}-Mal) (NOF Corporation, Tokyo, Japan) in a molar ratio of 2:9:0.57, followed by incubation for 10 min at room temperature to hydrate the lipids. The solution was sonicated for 5 min in a bath-type sonicator (42 kHz, 100 W) (2510J-DTH; Bransonic Ultrasonic Co., Danbury, CT). For coupling, TAT peptide, at a molar ratio of 5-fold DSPE-PEG_{2000}-Mal, was added to the PEG liposomes, and the mixture was incubated for 6 h at room temperature to conjugate the cysteine of the Cys-TAT peptide with the maleimide of the PEG liposomes using a thioether bond. The resulting TAT-peptide conjugated PEG liposomes (TAT-PEG liposomes) were dialyzed to remove any excess peptide. TAT-PEG liposomes were modified with 5 mol % PEG and 3 mol % peptides of total lipid. The particle size and ζ-potential of prepared liposomes were measured by NICOMP 380 ZLS (Particle Sizing Systems, Santa Barbara, CA).

Preparation of Bubble Liposomes. PEG liposomes composed of 1,2-dipalmitoyl-*sn*-glycero-3-phosphocholine (DPPC) (NOF Corporation) and 1,2-distearoyl-*sn*-glycero-3-phosphatidylethanolamine-poly(ethylene glycol) (DSPE-PEG_{2000}-OMe) (NOF Corporation) in a molar ratio of 94:6 were prepared by the reverse-phase evaporation method. In brief, all reagents were dissolved in 1:1 (v/v) chloroform/diisopropyl ether. Phosphate-buffered saline was added to the lipid solution, and the mixture was sonicated and then evaporated at 47 °C. The organic solvent was completely removed, and the size of the liposomes was adjusted to less than 200 nm using extruding equipment and a sizing filter (pore size: 200 nM) (Nuclepore Track-Etch Membrane; Whatman Plc, UK). The lipid concentration was measured using a phospholipid C test Wako (Wako Pure Chemical Industries, Ltd., Osaka, Japan). BLs were prepared from liposomes and perfluoropropane gas (Takachio Chemical Ind. Col. Ltd., Tokyo, Japan). First, 2 mL sterilized vials containing 0.8 mL of liposome suspension (lipid concentration: 1 mg/mL) were filled with perfluoropropane gas, capped, and then pressurized with a further 3 mL of perfluoropropane gas. The vial was placed in a bath-type sonicator (42 kHz, 100 W) (2510j-DTH; Branson Ultrasonics Co.) for 5 min to form BLs.

Transfection of pDNA into Cells Using TAT-PEG Liposomes. The day before the experiments, HeLa cells (3×10^4) were seeded in a 48-well plate. The cells were treated with TAT-PEG liposomes (encapsulated pDNA: 3 μg/mL) in serum-free medium for 4 h at 37 °C. After replacement with fresh medium, the cells were cultured for 20 h, and then luciferase activity was measured.

Transfection of pDNA into Cells by Combination of TAT-PEG Liposomes with BLs and US Exposure. The day before the experiments, HeLa cells (3×10^4) were seeded in a 48-well plate. The cells were treated with TAT-PEG liposomes (encapsulated pDNA: 3 μg/mL) in serum-free medium for 4 h at 37 °C. After incubation, the cells were washed twice within 10 min to remove any excess TAT-PEG liposomes that were not associated with the cells, and BLs (120 μg/mL) were added. Within 2 min, US exposure was applied through a 6 mm diameter probe placed in the well (frequency, 2 MHz; duty, 50%; burst rate, 2 Hz; intensity, 1.0 W/cm^2; time, 10 s). A Sonopore 3000 (NEPA GENE Co. Ltd., Chiba, Japan) was used to generate the US exposure. The cells were cultured for 20 h; then luciferase activity was determined, and cell viability was measured using a WST-8 assay (Cell Counting Kit-8; Dojindo Laboratories, Kumamoto, Japan).

Measurement of Luciferase Expression. Cell lysate was prepared with lysis buffer (0.1 M Tris-HCl (pH 7.8), 0.1% Triton X-100, and 2 mM EDTA). Luciferase activity was measured using a luciferase assay system (Promega) and a luminometer (LB96 V; Berthold Japan Co. Ltd., Tokyo, Japan). Activity is indicated as relative light units (RLU) per milligrams of protein.

Flow Cytometry Analysis. The day before the experiments, HeLa cells were seeded in a 12-well plate. Then, 0.2 mol % DiI-labeled TAT-PEG liposomes (pDNA: 3 μg/mL) were added to the cells and incubated for 1 h at 37 °C. The cells were collected, and the fluorescence intensities were measured by flow cytometry (FACSCanto; BD Biosciences, Franklin Lakes, NJ) to evaluate the cellular association of liposomes.

To examine the effect of BLs and US exposure on cellular uptake of pDNA, TAT-PEG liposomes (encapsulating Cy3-labeled pDNA: 3 μg/mL) were added to cells and incubated for 4 h at 37 °C. After incubation, the cells were washed twice, and BLs (120 μg/mL) were added. Then, US exposure was applied (frequency, 2 MHz; duty, 50%; burst rate, 2 Hz; intensity, 1.0 W/cm^2; time, 10 s). Subsequently, the cells were incubated for 10 or 60 min, and then the cells were collected by trypsinization and washed with PBS supplemented with heparin (50 μg/mL) three times to remove TAT-PEG liposomes and pDNA bound to the cell surface. The fluorescence intensity was measured by flow cytometry.

Confocal Laser Scanning Microscopy (CLSM). HeLa cells were seeded a day before the experiments. HeLa cells were

dx.doi.org/10.1021/mp200353m | *Mol. Pharmaceutics* 2011, 8, 2416–2423

treated with TAT-PEG liposomes (Cy3-labeled pDNA: 3 μg/mL) and FITC-CTB (10 μg/mL) for 1 h at 37 °C. After incubation, the cells were washed, and BLs (120 μg/mL) were added. US exposure was then applied (frequency, 2028 kHz; duty, 50%; burst rate, 2.0 Hz; intensity, 1.0 W/cm^2; time, 10 s). Subsequently, the cells were incubated for 10, 60, or 180 min and then fixed with 4% paraformaldehyde for 1 h at 4 °C. CLSM was then performed (FV1000D; Olympus Corporation, Tokyo, Japan).

RESULTS

Characterization of Prepared TAT-PEG Liposomes. We evaluated the average size and zeta potential of prepared TAT-PEG liposomes, which were about 130 nm with a slight positive charge (Table 1).

Table 1. Characteristics of Prepared Liposomes[a]

prepared liposomes	PEG liposomes	TAT-PEG liposomes
particle size (nm)	132.1 ± 6.5	122.5 ± 10.5
ζ potential (mV)	3.17 ± 1.7	7.91 ± 1.6

[a]Data are the means and SD of three different determinations.

Cellular Association of TAT-PEG Liposomes. We first confirmed the effect of TAT peptide coating on the cellular association of liposomes and examined the association of TAT-PEG liposomes with HeLa cells. The cells were incubated with DiI-labeled liposomes for 1 h at 37 °C, and fluorescence intensity was determined by flow cytometry. The cellular internalization of TAT-PEG liposomes was observed by confocal laser scanning microscopy (CLSM). The cells treated with TAT-PEG liposomes showed increased fluorescence intensities compared with nonlabeled PEG liposomes (Figure 1A). In cells treated with TAT-PEG liposomes, the fluorescence of liposomes was observed in the cytoplasm, whereas it was weak in the cytoplasm of cells treated with nonlabeled PEG liposomes (Figure 1B). Furthermore, we investigated the cellular uptake pathway of TAT-PEG liposomes. Inhibitors that block clathrin-mediated endocytosis, raft-dependent endocytosis, and macropinocytosis were used to determine the cellular uptake pathway of TAT-PEG liposomes. Clathrin-mediated endocytosis was inhibited by chlorpromazine, which prevents the assembly of coated pits at the plasma membrane.[15] Raft-dependent endocytosis was inhibited by genistein, which is a thyrosine

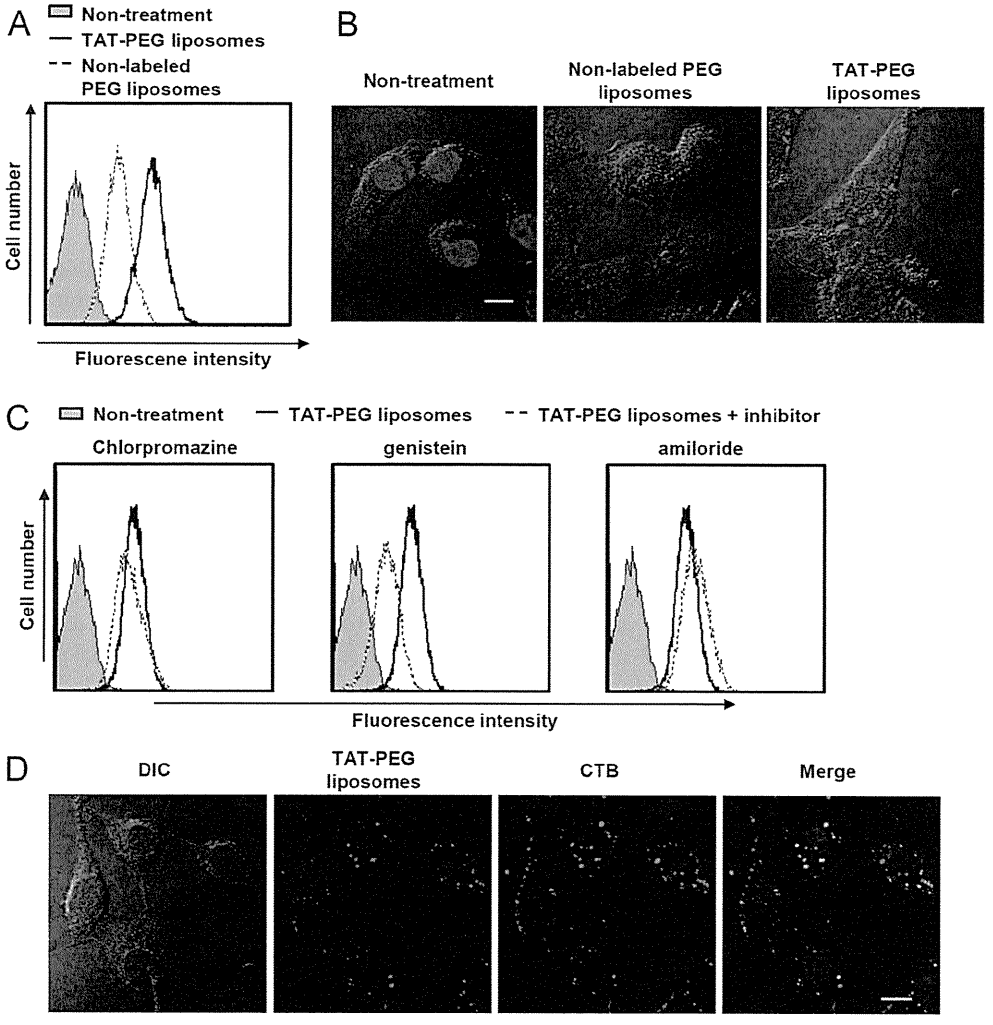

Figure 1. Cellular association of TAT-PEG liposomes. (A, B) HeLa cells were treated with DiI-labeled nonlabeled or TAT-PEG liposomes for 1 h at 37 °C. (A) The fluorescence intensity was measured by flow cytometry. (B) Cells were observed by CLSM. The scale bar represents 10 μm. (C) Cells were incubated with chlorpromazine (10 μg/mL), genistein (400 μM), or amiloride (1 mM) for 30 min and then treated with DiI-labeled TAT-PEG liposomes in the presence of an endocytic inhibitor for a further 1 h at 37 °C. Fluorescence intensities were measured by flow cytometry. (D) Cells were treated with DiI-labeled nonlabeled or TAT-PEG liposomes in the presence of FITC-CTB (10 μg/mL) for 1 h at 37 °C. Cells were observed by CLSM. The scale bar represents 10 μm.

kinase inhibitor.[16] We also used amiloride, a specific inhibitor of the Na^+/H^+ exchange required for macropinocytosis.[17] Flow cytometry analysis showed that the fluorescence intensity of TAT-PEG liposomes in the cells was decreased when cells were treated with genistein. In contrast, the fluorescence intensity of TAT-PEG liposomes in the cells was not changed when cells were treated with chlorpromazine or amiloride (Figure 1C). Furthermore, to elucidate the intracellular localization of TAT-PEG liposomes, the cells were treated with DiI-labeled TAT-PEG liposomes and FITC-cholera toxin B subunit (FITC-CTB), a marker of raft-dependent endocytosis,[18] and then observed by CLSM. As a result, the fluorescence of TAT-PEG liposomes was colocalized with the fluorescence of CTB in cells treated with TAT-PEG liposomes and CTB for 1 h (Figure 1D).

Gene Transfection by TAT-PEG Liposomes. Although TAT-PEG liposomes could be internalized efficiently into cells via raft-dependent endocytosis, it was necessary to achieve high gene expression so that genes in the endosome were delivered into the cytoplasm. To assess the ability of endosomal escape in TAT-PEG liposomes, the cells were treated with TAT-PEG liposomes in the presence of chloroquine, which is recognized as an endosomolytic agent.[19] Luciferase activity was 100-fold higher than that following treatment with TAT-PEG liposomes in the absence of chloroquine (Figure 2). It was suggested that

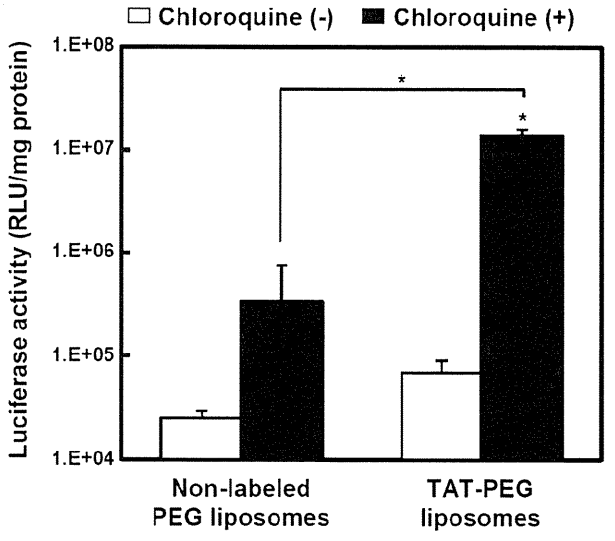

Figure 2. Gene transfection by TAT-PEG liposomes. Cells were preincubated with chloroquine (100 μM) for 30 min before transfection and then treated with nonlabeled or TAT-PEG liposomes in the presence of chloroquine for a further 4 h at 37 °C. After replacement with fresh medium, the cells were cultured for 20 h, and then luciferase activity was determined. Scale bars represent 10 μm. Data are the means ± SD ($n = 4$). *$p < 0.05$ compared with treatment in the absence of chloroquine.

the TAT-PEG liposomes prepared in this study could be efficiently internalized into cells but might not release genes into the cytoplasm from endosomes.

Effects of BLs and US Exposure on the Transfection Efficiency of TAT-PEG Liposomes. To investigate the effect of BLs and US exposure on TAT-mediated liposomal gene transfection, HeLa cells were treated with TAT-PEG liposomes for 4 h at 37 °C in a serum-free medium, and then the cells were treated with BLs and US exposure. After treatment with TAT-PEG liposomes, luciferase activity was enhanced up to 30-fold by BLs and US exposure compared with TAT-PEG liposomes alone. Furthermore, the combination of TAT-PEG liposomes with BLs and US exposure had about 10-fold higher luciferase activity than nonlabeled PEG liposomes with BLs and US exposure (Figure 3A). We also examined the transfection efficiency by treating TAT-PEG liposomes with US in the absence of BLs. As a result, the transfection efficiency was barely enhanced by treatment with TAT-PEG liposomes with US compared with TAT-PEG liposomes alone (Figure 3B). The cytotoxicity of the combination of TAT-PEG liposomes with or without BLs and US exposure was determined using a WST-8 assay. The cell viability was more than 80% even after each transfection (Figure 3C,D). It was suggested that BLs and US exposure could enhance the transfection efficiency of TAT-PEG liposomes without significant cytotoxicity.

Mechanism of Gene Transfection by TAT-PEG Liposomes with BLs and US Exposure. We examined the effects of BLs and US exposure on the cellular uptake of TAT-PEG liposomes. Flow cytometry analysis was performed to measure the fluorescence intensity of Cy3-labeled pDNA in cells transfected by TAT-PEG liposomes with or without BLs and US exposure. As a result, the cellular uptake of pDNA showed almost no difference in the presence of TAT-PEG liposomes with or without BLs and US exposure (Figure 4A). To evaluate the involvement of the direct induction of TAT-PEG liposomes into cells, the cells were transfected with TAT-PEG liposomes with or without BLs and US exposure at 37 or 4 °C. Twenty-three hours after transfection, luciferase activity was measured. When the cells were transfected by TAT-PEG liposomes with BLs and US exposure at 37 °C, the luciferase activity increased compared with that of cells treated with TAT-PEG liposomes alone. In contrast, luciferase activity did not change in cells treated with TAT-PEG liposomes with BLs and US exposure at 4 °C compared with TAT-PEG liposomes alone (Figure 4B). We also confirmed the effect of temperature on the cellular uptake of TAT-PEG liposomes. The cells were treated with DiI-labeled TAT-PEG liposomes for 1 h at 37 °C or at 4 °C, and then fluorescence intensity was measured by flow cytometry. In cells treated at 4 °C, fluorescence intensity decreased compared with cells treated at 37 °C (data not shown). To evaluate the intracellular distribution of pDNA, HeLa cells were treated with TAT-PEG liposomes containing Cy3-labeled pDNA in the presence of FITC-CTB for 1 h, and then the cells were treated with BLs and US exposure. After US exposure, the cells were incubated for 10, 60, or 180 min and observed by CLSM. In cells treated with TAT-PEG liposomes alone, the fluorescence of pDNA colocalized with the fluorescence of CTB. In contrast, when cells were treated with BLs and US exposure, the fluorescence of CTB was dispersed widely in cells that were incubated for 10 min after US exposure (Figure 4C). We also confirmed the intracellular distribution of pDNA and CTB in living cells. As a result, the distribution of pDNA and CTB in living cells was similar to that of fixed cells (data not shown). Furthermore, we examined the intracellular distribution of pDNA and CTB treated by TAT-PEG liposomes with US in the absence of BLs. The intracellular distribution of pDNA and CTB showed almost no difference between the treatment of TAT-PEG liposomes alone and TAT-PEG liposomes with US exposure without BLs (data not shown).

It was suggested that BLs and US exposure could affect the intracellular trafficking of pDNA and enhance the transfection efficacy of TAT-PEG liposomes.

dx.doi.org/10.1021/mp200353m | *Mol. Pharmaceutics* 2011, 8, 2416–2423

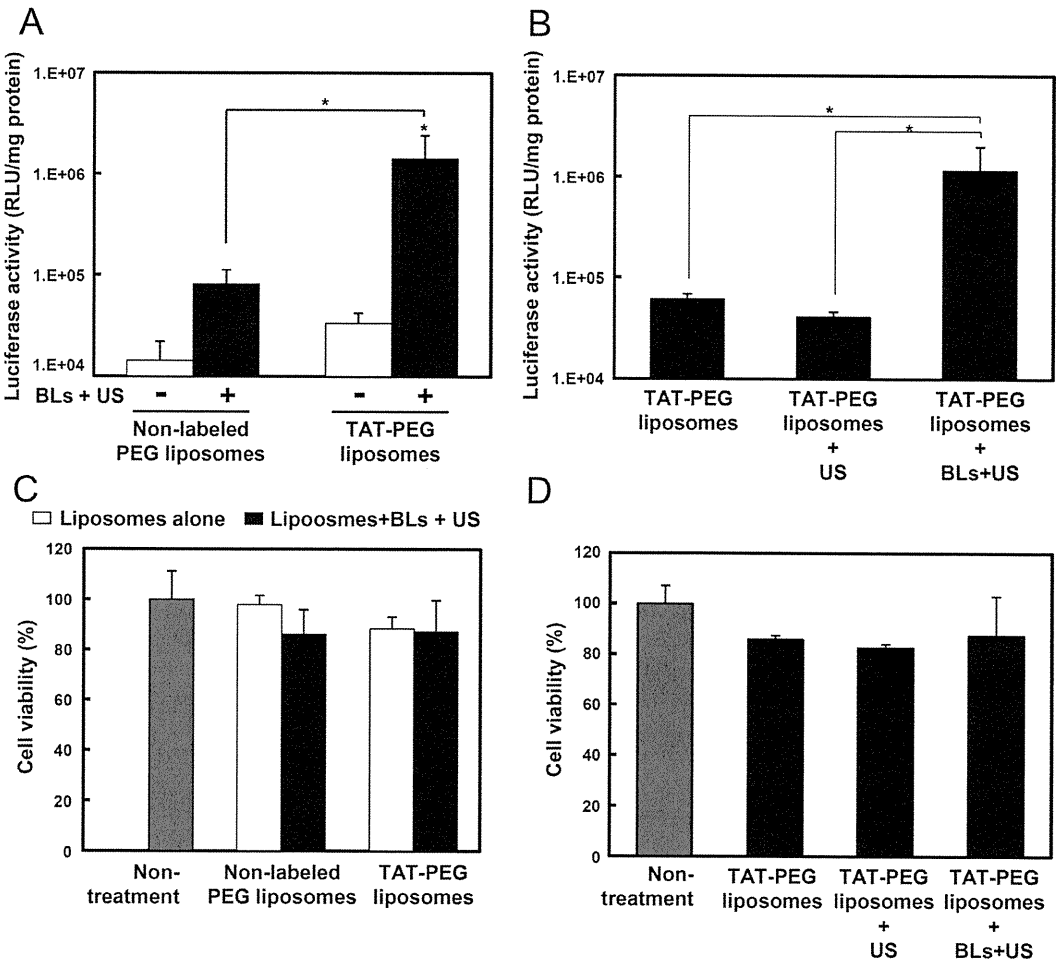

Figure 3. Effect of BLs and US exposure on TAT-mediated liposomal gene transfection. HeLa cells were treated with nonlabeled or TAT-PEG liposomes for 4 h. The cells were then washed and treated with or without BLs (120 μg/mL) and US exposure. They were incubated for 20 h; then (A, B) luciferase activity was determined, and (C, D) cell viability was measured using a WST-8 assay. Data are the means ± SD (n = 4). *p < 0.05 compared with TAT-PEG liposomes alone.

DISCUSSION

Recent studies have suggested that endosomal escape is important to achieve efficient gene delivery.[2,3] We have previously reported that BLs and US exposure could improve the transfection efficiency of laminin-derived AG73-PEG liposomes containing pDNA by promoting endosomal escape.[9] In this report, we demonstrated that BLs and US exposure could enhance not only the transfection efficiency of AG73-PEG liposomes but also that of TAT-PEG liposomes.

For efficient gene delivery, various moieties were used to develop carriers which enhance cellular internalization or selectivity. CPPs, such as TAT, R8, or penetratin, were used to achieve efficient gene internalization.[12,20,21] On the other hand, for selective gene delivery, folate, transferrin, RGD, or anisamide was used as a ligand.[22−25] These moieties were associated with a specific receptor and internalized via several endocytoses. TAT peptide was associated with heparan sulfate proteoglycan, which has been controversial.[26] In addition, some studies have developed TAT peptide-modified carriers, which were equipped with components enhancing endosomal escape;[14] therefore, we focused on TAT peptide and evaluated whether BLs and US exposure can enhance the transfection efficiency of TAT peptide-modified carriers to demonstrate the utility of BLs and US exposure in general. The present results showed that BLs and US exposure could enhance the gene transfection efficiency of TAT-PEG liposomes (Figure 3A). Furthermore, although we have previously reported that AG73-PEG liposomes were partially internalized via clathrin-mediated endocytosis,[9] the TAT-PEG liposomes prepared in this study were mostly internalized via a raft-dependent endocytic pathway (Figure 1C). These results suggested that BLs and US exposure could enhance the transfection efficiency of vectors, which were internalized via various receptor and endocytic pathways; however, further studies are needed to evaluate the effect of BLs and US exposure on the transfection efficiency of vectors, which were internalized via various endocytic pathways, such as macropinocytosis.

For successful gene therapy, nonviral vectors could be needed to overcome rate-limiting steps, such as cellular internalization, endosomal escape, and nuclear transfer.[2,3] Endosomal escape is considered to be one of the most important steps. Although PEG modification was considered a useful component to increase the stability of vectors in vivo, it also inhibited endosomal escape, leading to decreased gene expression.[27,28] Our results also showed that TAT-PEG liposomes could not escape from endosomes to the cytosol efficiently (Figures 1D, 2). We previously reported that BLs and US exposure could enhance the endosomal escape of AG73-PEG liposomes.[9] We therefore further confirmed the effect of BLs and US exposure on endosomal escape of TAT-PEG liposomes. We and other

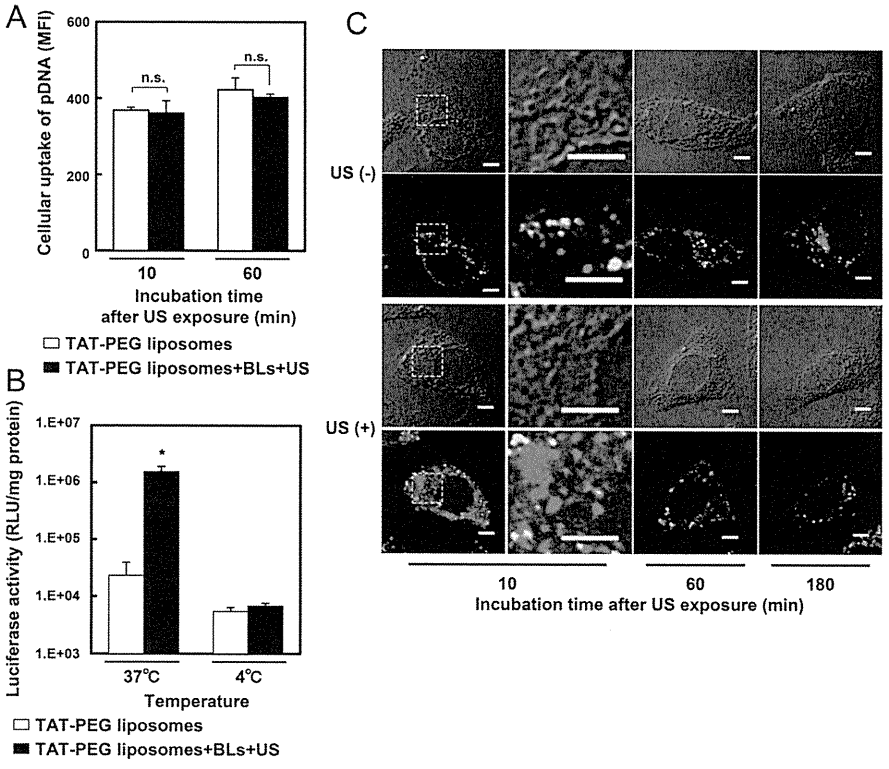

Figure 4. Mechanism of accelerated TAT-mediated liposomal gene transfection by BLs and US exposure. (A) HeLa cells were incubated with TAT-PEG liposomes encapsulating Cy3-labeled pDNA for 4 h at 37 °C. After incubation, the cells were washed, and BLs were added. Then the cells were exposed to US and incubated for 10 or 60 min. The cells were then collected and washed with heparin-containing PBS three times. The fluorescence intensity was measured by flow cytometry. Data are shown as the means ± SD (n = 3). (B) Cells were preincubated for 30 min at either 37 or 4 °C before transfection and then treated with TAT-PEG liposomes for a further 1 h at 37 or 4 °C. After incubation, the cells were washed, and BLs were added. The cells were then exposed to US and cultured for 23 h. Luciferase activity was determined. Data are the means ± SD (n = 4). *p < 0.05 compared with TAT-PEG liposomes alone. (C) Cells were treated with TAT-PEG liposomes encapsulating Cy3-labeled pDNA and FITC-CTB (10 μg/mL) for 1 h at 37 °C. After incubation, the cells were washed, and BLs were added. The cells were then exposed to US, incubated for 10, 60, 180 min, and then fixed with 4% paraformaldehyde for 1 h at 4 °C and observed by CLSM. The areas surrounded by dotted line are shown as enlarged images. Scale bars represent 5 μm.

groups have reported that the combination of BLs or microbubbles with US exposure could increase cell membrane permeability and deliver genes into the cytosol directly;[29−33] however, our results indicated that enhanced transfection efficiency did not rely on the increase of the direct cellular uptake of TAT-PEG liposomes, which is associated with the cell membrane (Figure 4A). In addition, CLSM analysis showed that BLs and US exposure could affect intracellular trafficking of TAT-PEG liposomes. Although endocytic vesicles labeled with FITC-CTB were observed as punctuate structures, when BLs and US exposure was applied, it was observed that FITC-CTB diffused into the cytosol (Figure 4B). These results suggested that BLs and US exposure could accelerate endosomal escape of TAT-PEG liposomes. We also examined whether sonazoid (Daiichi-Sankyo Pharmaceuticals, Tokyo, Japan) and US exposure could enhance the transfection efficiency of TAT-PEG liposomes. Sonazoid consists of perfluorobutane gas microbubbles stabilized by a monolayer membrane of hydrogenated egg phosphatidyl serine.[34] As a result, the transfection efficiency of TAT-PEG liposomes was enhanced by sonazaoid and US exposure (data not shown). This result suggested that microbubbles and US exposure could enhance the gene transfection efficiency of gene delivery carriers.

We also prepared folate-PEG liposomes containing pDNA and examined whether BLs and US exposure could enhance the transfection efficiency of folate-PEG liposomes. Folate, a high-affinity ligand for folate receptor, has been widely used as a ligand for selective gene delivery, and folate-modified carriers required various components enhancing endosomal escape to achieve high gene transfection efficiency.[35] We confirmed that folate-PEG liposomes had relatively low transfection efficiency because of the lower ability of endosomal escape, but when BLs and US exposure was used with folate-PEG liposomes, the transfection efficiency of folate-PEG lisposomes was enhanced (data not shown). These findings also suggested that BLs and US exposure could enhance the endosomal escape of gene delivery vectors, leading to increased gene expression.

We have reported that the transfection efficiency of AG73-PEG liposomes using BLs and US exposure was enhanced 60-fold,[9] whereas that of TAT-PEG liposomes was up-regulated 12-fold (Figure 3A). These results suggested that BLs and US exposure could easily influence the intracellular trafficking of AG73-PEG liposomes compared to TAT-PEG liposomes. The different efficacy of endosomal escape between AG73-PEG liposomes and TAT-PEG liposomes might be dependent on the difference of the receptor, endocytic pathway of carrier, and the type of cells. The responsibility of BLs and US exposure to individual cells might also affect the efficiency of endosomal escape, leading to different transfection efficiencies; therefore, it is important to clarify the mechanism of the different efficacy of endosomal escape of these carriers. However, we expect that this method of promoting endosomal escape using BLs and US

dx.doi.org/10.1021/mp200353m | Mol. Pharmaceutics 2011, 8, 2416–2423

exposure may also be applied to existing carriers for drug, peptide, or protein delivery, which have low intracellular delivery efficacy due to poor endosomal escape.

In further studies, we will attempt to demonstrate the detailed mechanism of enhanced endosomal escape of carriers by treatment with BLs and US exposure. It has been demonstrated that microbubbles and US exposure induce several biological effects, such as influx of calcium ions or generation of reactive oxygen species.[36−39] It has been also reported that endosomal acidification is adjusted by calcium ions;[40] therefore, we will assess whether the influx of calcium ions induced by BLs and US exposure affects endosomal acidification and function, leading to the destabilization of endosomes and enhancement of endosomal escape. On the other hand, we may also need to elucidate more clearly the effect of BLs and US exposure on transcription and other organelles. Although it is possible that BLs and US exposure may induce several biological effects involved in gene expression, BLs and US exposure could affect the intracellular distribution of pDNA and CTB (Figure 4); therefore, our results suggested that BLs and US exposure could certainly improve at least the endosomal escape of TAT-PEG liposomes.

In conclusion, as schematically shown in Figure 5, TAT-PEG liposomes were internalized into cells via HSPG and raft-dependent endocytosis. On the other hand, AG73-PEG liposomes and folate-PEG liposomes were internalized via syndecan-2 and folate receptor, respectively. When BLs and US exposure were applied, endosomal escape was enhanced, leading to increased transfection efficiency of these carriers. These results suggested that BLs and US exposure could enhance transfection efficiency by promoting endosomal escape, which was independent of the receptors and endocytic pathway of carriers. Thus, BLs and US exposure can be useful tools to achieve efficient gene transfection by improving endosomal escape using various carriers.

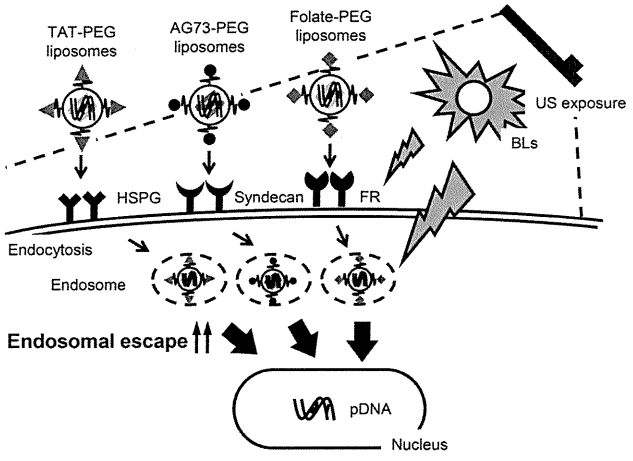

Figure 5. Diagram of enhanced gene delivery by BLs and US exposure. Several moiety-modified gene delivery carriers were internalized into cells via receptors and the endocytic pathway. When BLs and US exposure were applied, endosomal escape was enhanced, leading to increased transfection efficiency, which was independent of the receptor and endocytic pathway of carriers. HSPG, heparan sulfate proteoglycan; FR, folate receptor; US, ultrasound; BLs, Bubble liposomes; PEG, poly(ethylene glycol).

AUTHOR INFORMATION

Corresponding Author

*Mailing address: Tokyo University of Pharmacy and Life Sciences, School of Pharmacy, 1432-1 Horinouchi, Hachioji, Tokyo 192-0392, Japan. Tel. and fax: +81-42-676-3183. E-mail address: negishi@toyaku.ac.jp (Y.N.).

ACKNOWLEDGMENTS

We are grateful to Dr. Katsuro Tachibana (Department of Anatomy, School of Medicine, Fukuoka University) for technical advice regarding the induction of cavitation with US and to Mr. Yasuhiko Hayakawa, Mr. Takahiro Yamauchi, and Mr. Kosho Suzuki (NEPA GENE CO., LTD.) for technical advice regarding exposure to US. This study was supported by an Industrial Technology Research Grant (04A05010) from the New Energy and Industrial Technology Development Organization (NEDO) of Japan, Grant-in-Aid for Exploratory Research (18650146) and Grant-in-Aid for Scientific Research (B) (20300179) from the Japan Society for the Promotion of Science, and by a grant for private universities provided by the Promotion and Mutual Aid Corporation for Private Schools of Japan.

ABBREVIATIONS

BLs, Bubble liposomes; CTB, cholera toxin B subunit; DOPE, 1,2-dioleoyl-sn-glycero-3-phosphoethanolamine; DOPG, 1,2-dioleoyl-*sn*-glycero-3-phospho-*rac*-1-glycerol; DSPE, 1,2-distearoyl-*sn*-glycero-3-phosphatidyl-ethanolamine; FBS, fetal bovine serum; Fmoc, fluorenylmethoxycarbonyl; Mal, maleimide; pDNA, plasmid DNA; PEG, poly(ethylene glycol); US, ultrasound

REFERENCES

(1) Zhang, S.; Xu, Y.; Wang, B.; Qiao, W.; Liu, D.; Li, Z. Cationic compounds used in lipoplexes and polyplexes for gene delivery. *J. Controlled Release* **2004**, *100*, 165−180.

(2) Hama, S.; Akita, H.; Ito, R.; Mizuguchi, H.; Hayakawa, T.; Harashima, H. Quantitative comparison of intracellular trafficking and nuclear transcription between adenoviral and lipoplex systems. *Mol. Ther.* **2006**, *13*, 786−794.

(3) Varga, C. M.; Tedford, N. C.; Thomas, M.; Klibanov, A. M.; Griffith, L. G.; Auffenburger, D. A. Quantitative comparison of polyethylenimine formulations and adenoviral vectors in terms of intracellular gene delivery processes. *Gene Ther.* **2005**, *12*, 1023−1032.

(4) Hatakeyama, H.; Ito, E.; Akita, H.; Oishi, M.; Nagasaki, Y.; Futaki, S.; Harashima, H. A pH-sensitive fusogenic peptide facilitates endosomal escape and greatly enhances the gene silencing of siRNA-containing nanoparticles in vitro and in vivo. *J. Controlled Release* **2009**, *139*, 127−132.

(5) Subbarao, N. K.; Parente, R. A.; Szoka, F. C.; Nadasdi, L.; Pongracz, K. pH-dependent bilayer destabilization by an amphipathic peptide. *Biochemistry* **1987**, *26*, 2964−2972.

(6) Lee, S. H.; Choi, S. H.; Kim, S. H.; Park, T. G. Thermally sensitive cationic polymer nanocapsules for specific cytosolic delivery and efficient gene silencing of siRNA: swelling induced physical disruption of endosome by cold shock. *J. Controlled Release* **2008**, *125*, 25−32.

(7) Høgset, A.; Prasmickaite, L.; Selbo, P. K.; Hellum, M.; Engesaeter, B. Ø.; Bonsted, A.; Berg, K. Photochemical internalisation in drug and gene delivery. *Adv. Drug Delivery Rev.* **2004**, *56*, 95−115.

(8) Negishi, Y.; Omata, D.; Iijima, H.; Hamano, N.; Endo-Takahashi, Y.; Nomizu, M.; Aramaki, Y. Preparation and characterization of laminin-derived peptide AG73-coated liposomes as a selective gene delivery tool. *Biol. Pharm. Bull.* **2010**, *33*, 1766−1769.

(9) Negishi, Y.; Omata, D.; Iijima, H.; Takabayashi, Y.; Suzuki, K.; Endo, Y.; Suzuki, R.; Maruyama, K.; Nomizu, M.; Aramaki, Y. Enhanced laminin-derived peptide AG73-mediated liposomal gene transfer by Bubble liposomes and ultrasound. *Mol. Pharmaceutics* **2010**, *7*, 217–226.

(10) Katayama, S.; Hirose, H.; Takayama, K.; Nakase, I.; Futaki, S. Acylation of octaarginine: Implication to the use of intracellular delivery vectors. *J. Controlled Release* **2011**, *149*, 29–35.

(11) Dey, D.; Inayathullah, M.; Lee, A. S.; Lemieux, M. C.; Zhang, X.; Wu, Y.; Nag, D.; De Almeida, P. E.; Han, L.; Rajadas, J.; Wu, J. C. Efficient gene delivery of primary human cells using peptide linked polyethylenimine polymer hybrid. *Biomaterials* **2011**, *32*, 4647–4658.

(12) Yamano, S.; Dai, J.; Yuvienco, C.; Khapli, S.; Moursi, A. M.; Montclare, J. K. Modified Tat peptide with cationic lipids enhances gene transfection efficiency via temperature-dependent and caveolae-mediated endocytosis. *J. Controlled Release* **2011**, *152*, 278–285.

(13) Zeng, X.; Sun, Y. X.; Qu, W.; Zhang, X. Z.; Zhuo, R. X. Biotinylated transferrin/avidin/biotinylated disulfide containing PEI bioconjugates mediated p53 gene delivery system for tumor targeted transfection. *Biomaterials* **2010**, *31*, 4771–4780.

(14) Suk, J. S.; Suh, J.; Choy, K.; Lai, S. K.; Fu, J.; Hanes, J. Gene delivery to differentiated neurotypic cells with RGD and HIV Tat peptide functionalized polymeric nanoparticles. *Biomaterials* **2006**, *27*, 5143–5150.

(15) Wang, L. H.; Rothberg, K. G.; Anderson, R. G. Mis-assembly of clathrin lattices on endosomes reveals a regulatory switch for coated pit formation. *J. Cell. Biol.* **1993**, *123*, 1107–1117.

(16) Pelkmans, L.; Püntener, D.; Helenius, A. Local actin polymerization and dynamin recruitment in SV40-induced internalization of caveolae. *Science* **2002**, *296*, 535–539.

(17) Wadia, J. S.; Stan, R. V.; Dowdy, S. F. Transducible TAT-HA fusogenic peptide enhances escape of TAT-fusion proteins after lipid raft macropinocytosis. *Nat. Med.* **2004**, *10*, 310–315.

(18) Janes, P. W.; Ley, S. C.; Magee, A. I. Aggregation of lipid rafts accompanies signaling via the T cell antigen receptor. *J. Cell. Biol.* **1999**, *147*, 447–461.

(19) Sonawane, N. D.; Szoka, F. C.; Verkman, A. S. Chloride accumulation and swelling in endosomes enhances DNA transfer by polyamine-DNA polyplexes. *J. Biol. Chem.* **2003**, *278*, 44826–44831.

(20) Kibria, G.; Hatakeyama, H.; Ohga, N.; Hida, K.; Harashima, H. Dual-ligand modification of PEGylated liposomes shows better cell selectivity and efficient gene delivery. *J. Controlled Release* **2011**, *153*, 141–148.

(21) Mäe, M.; El Andaloussi, S.; Lundin, P.; Oskolkov, N.; Johansson, H. J.; Guterstam, P.; Langel, U. A stearylated CPP for delivery of splice correcting oligonucleotides using a non-covalent co-incubation strategy. *J. Controlled Release* **2009**, *134*, 221–227.

(22) Morris, V. B.; Sharma, C. P. Folate mediated l-arginine modified oligo (alkylaminosiloxane) graft poly(ethyleneimine) for tumor targeted gene delivery. *Biomaterials* **2011**, *32*, 3030–3041.

(23) Koppu, S.; Oh, Y. J.; Edrada-Ebel, R.; Blatchford, D. R.; Tetley, L.; Tate, R. J.; Dufes, C. Tumor regression after systemic administration of a novel tumor-targeted gene delivery system carrying a therapeutic plasmid DNA. *J. Controlled Release* **2010**, *143*, 215–221.

(24) Ng, Q. K.; Sutton, M. K.; Soonsawad, P.; Xing, L.; Cheng, H.; Segura, T. Engineering clustered ligand binding into nonviral vectors: $\alpha v\beta 3$ targeting as an example. *Mol. Ther.* **2009**, *17*, 828–836.

(25) Li, S. D.; Chono, S.; Huang, L. Efficient oncogene silencing and metastasis inhibition via systemic delivery of siRNA. *Mol. Ther.* **2008**, *16*, 942–946.

(26) Imamura, J.; Suzuki, Y.; Gonda, K.; Roy, C. N.; Gatanaga, H.; Ohuchi, N.; Higuchi, H. Single Particle Tracking Confirms That Multivalent Tat Protein Transduction Domain-induced Heparan Sulfate Proteoglycan Cross-linkage Activates Rac1 for Internalization. *J. Biol. Chem.* **2011**, *286*, 10581–10592.

(27) Hatakeyama, H.; Akita, H.; Kogure, K.; Oishi, M.; Nagasaki, Y.; Kihira, Y.; Ueno, M.; Kobayashi, H.; Kikuchi, H.; Harashima, H. Development of a novel systemic gene delivery system for cancer therapy with a tumor-specific cleavable PEG-lipid. *Gene Ther.* **2007**, *14*, 68–77.

(28) Walker, G. F.; Fella, C.; Pelisek, J.; Fahrmeir, J.; Boeckle, S.; Ogris, M.; Wagner, E. Toward synthetic viruses: endosomal pH-triggered deshielding of targeted polyplexes greatly enhances gene transfer in vitro and in vivo. *Mol. Ther.* **2005**, *11*, 418–425.

(29) Negishi, Y.; Matsuo, K.; Endo-Takahashi, Y.; Suzuki, K.; Matsuki, Y.; Takagi, N.; Suzuki, R.; Maruyama, K.; Aramaki, Y. Delivery of an angiogenic gene into ischemic muscle by novel Bubble liposomes followed by ultrasound exposure. *Pharm. Res.* **2011**, *28*, 712–719.

(30) Suzuki, R.; Namai, E.; Oda, Y.; Nishiie, N.; Otake, S.; Koshima, R.; Hirata, K.; Taira, Y.; Utoguchi, N.; Negishi, Y.; Nakagawa, S.; Maruyama, K. Cancer gene therapy by IL-12 gene delivery using liposomal bubbles and tumoral ultrasound exposure. *J. Controlled Release* **2010**, *142*, 245–250.

(31) Lentacker, I.; Wang, N.; Vandenbroucke, R. E.; Demeester, J.; De Smedt, S. C.; Sanders, N. N. Ultrasound Exposure of Lipoplex Loaded Microbubbles Facilitates Direct Cytoplasmic Entry of the Lipoplexes. *Mol. Pharmaceutics* **2009**, *6*, 457–467.

(32) Negishi, Y.; Endo, Y.; Fukuyama, T.; Suzuki, R.; Takizawa, T.; Omata, D.; Maruyama, K.; Aramaki, Y. Delivery of siRNA into the cytoplasm by liposomal bubbles and ultrasound. *J. Controlled Release* **2008**, *132*, 124–130.

(33) Taniyama, Y.; Tachibana, K.; Hiraoka, K.; Aoki, M.; Yamamoto, S.; Matsumoto, K.; Nakamura, T.; Ogihara, T.; Kaneda, T.; Morishita, R. Development of safe and efficient novel nonviral gene transfer using ultrasound: enhancement of transfection efficiency of naked plasmid DNA in skeletal muscle. *Gene Ther.* **2002**, *9*, 372–380.

(34) Otani, K.; Yamahara, K.; Ohnishi, S.; Obata, H.; Kitamura, S.; Nagaya, N. Nonviral delivery of siRNA into mesenchymal stem cells by a combination of ultrasound and microbubbles. *J. Controlled Release* **2009**, *133*, 146–153.

(35) Shi, G.; Guo, W.; Stephenson, S. M.; Lee, R. J. Efficient intracellular drug and gene delivery using folate receptor-targeted pH-sensitive liposomes composed of cationic/anionic lipid combinations. *J. Controlled Release* **2002**, *80*, 309–319.

(36) Juffermans, L. J.; Dijkmans, P. A.; Musters, R. J.; Visser, C. A.; Kamp, O. Transient permeabilization of cell membranes by ultrasound-exposed microbubbles is related to formation of hydrogen peroxide. *Am. J. Physiol. Heart Circ. Physiol.* **2006**, *291*, H1595–H1601.

(37) Juffermans, L. J.; Kamp, O.; Dijkmans, P. A.; Visser, C. A.; Musters, R. J. Low-intensity ultrasound-exposed microbubbles provoke local hyperpolarization of the cell membrane via activation of BK(Ca) channels. *Ultrasound Med. Biol.* **2008**, *34*, 502–508.

(38) Zhou, Y.; Shi, J.; Cui, J.; Deng, C. X. Effects of extracellular calcium on cell membrane resealing in sonoporation. *J. Controlled Release* **2008**, *126*, 34–43.

(39) Kumon, R. E.; Aehle, M.; Sabens, D.; Parikh, P.; Han, Y. W.; Kourennyi, D.; Deng, C. X. Spatiotemporal effects of sonoporation measured by real-time calcium imaging. *Ultrasound Med. Biol.* **2009**, *35*, 494–506.

(40) Lelouvier, B.; Puertollano, R. Mucolipin-3 regulates luminal calcium, acidification, and membrane fusion in the endosomal pathway. *J. Biol. Chem.* **2011**, *286*, 9826–9832.

Journal of Controlled Release 156 (2011) 355–363

Contents lists available at ScienceDirect

Journal of Controlled Release

journal homepage: www.elsevier.com/locate/jconrel

GENE DELIVERY

Involvement of activated transcriptional process in efficient gene transfection using unmodified and mannose-modified bubble lipoplexes with ultrasound exposure

Keita Un [a,b], Shigeru Kawakami [a,*], Yuriko Higuchi [c], Ryo Suzuki [d], Kazuo Maruyama [d], Fumiyoshi Yamashita [a], Mitsuru Hashida [a,e,*]

[a] Department of Drug Delivery Research, Graduate School of Pharmaceutical Sciences, Kyoto University, 46-29 Yoshida-Shimoadachi-cho, Sakyo-ku, Kyoto 606-8501, Japan
[b] The Japan Society for the Promotion of Science (JSPS), Chiyoda-ku, Tokyo 102-8471, Japan
[c] Institute for Innovative NanoBio Drug Discovery and Development, Graduate School of Pharmaceutical Sciences, Kyoto University, 46-29 Yoshida-Shimoadachi-cho, Sakyo-ku, Kyoto 606-8501, Japan
[d] Department of Biopharmaceutics, School of Pharmaceutical Sciences, Teikyo University, 1091-1 Suwarashi, Midori-ku, Sagamihara, Kanagawa 252-5195, Japan
[e] Institute for Integrated Cell-Material Sciences (iCeMS), Kyoto University, Yoshida-Ushinomiya-cho, Sakyo-ku, Kyoto 606-8302, Japan

ARTICLE INFO

Article history:
Received 6 May 2011
Accepted 27 June 2011
Available online 3 July 2011

Keywords:
Gene transfection
Bubble lipoplex
Ultrasound
Transcription factor
Inflammatory response

ABSTRACT

Recently, our group developed ultrasound (US)-responsive and mannose-modified gene carriers (Man-PEG_{2000} bubble lipoplexes), and successfully obtained a high level of gene expression in mannose receptor-expressing cells following gene transfection using Man-PEG_{2000} bubble lipoplexes and US exposure. We also reported that large amounts of plasmid DNA (pDNA) were transferred into the cytoplasm of the targeted cells in the gene transfection using this method. In the present study, we investigated the involvement of transcriptional processes on enhanced gene expression obtained by unmodified and Man-PEG_{2000} bubble lipoplexes with US exposure. The transcriptional process related to activator protein-1 (AP-1) and nuclear factor-κB (NFκB) was activated by US exposure, and was founded to be involved in enhanced gene expression obtained by gene transfection using unmodified and Man-PEG_{2000} bubble lipoplexes with US exposure. On the other hand, activation of AP-1 and NFκB pathways followed by US exposure was hardly involved in the inflammatory responses in the gene transfection using this method. These findings suggest that activation of AP-1 and NFκB followed by US exposure is involved in the enhanced gene expression using unmodified and Man-PEG_{2000} bubble lipoplexes with US exposure, and the selection of pDNAs activated by US exposure is important in this gene transfection method.

1. Introduction

Various obstacles are associated with in vivo gene transfection, including the control of in vivo distribution of nucleic acids, the improvement of intracellular/intranuclear transport of nucleic acids, and the activation of transcriptional/translational processes directly involved in the gene expression [1,2]. Viral and non-viral carriers have been studied as valuable gene carriers for in vivo gene transfection [3–6], with both possessing advantages and disadvantages relating to safety, productivity and gene expressing efficiency. Hama and Harashima et al. have reported that the high gene expression efficiency in gene transfection using viral carrier is influenced by the high transcriptional and translational efficiency following intranuclear transport of pDNA [7,8]. Therefore, the transcriptional/translational processes associated with gene transfection of non-viral carriers are potentially controlled by improved gene expression efficiency.

Gene transfection methods using physical stimulation, such as electroporation method [9], hydrodynamic injection [10,11], tissue pressure-mediated method [12] and sonoporation method [13], enable to obtain high-level gene expression. Gene expression has also been reported to be enhanced by intracytoplasmic transfer of pDNA as a result of using these methods [14–16]. Recently, our group developed US-responsive and/or mannose-modified gene carriers (unmodified and Man-PEG_{2000} bubble lipoplexes), and reported that high level gene expression can be selectively obtained in mannose receptor-expressing cells following intravenous administration of Man-PEG_{2000} bubble lipoplexes and US exposure, both in vitro and in vivo [17,18]. Furthermore, we have reported that large amounts of pDNA are transferred into the cytoplasm of targeted cells in the gene transfection using unmodified and Man-PEG_{2000} bubble lipoplexes with optimized US exposure under both in vitro and in vivo conditions [19].

Various types of physical stimulations, such as electric pulse, physical pressure, radiation and US exposure, can activate the transcriptional process involved in the AP-1-mediated and NFκB-

* Corresponding authors. Tel.: +81 75 753 4545; fax: +81 75 753 4575.
E-mail addresses: kawakami@pharm.kyoto-u.ac.jp (S. Kawakami), hashidam@pharm.kyoto-u.ac.jp (M. Hashida).

0168-3659/$ – see front matter © 2011 Elsevier B.V. All rights reserved.
doi:10.1016/j.jconrel.2011.06.040

mediated pathways [20–26]. It has been reported that this activation of transcription followed by physical stimulation partly contributes to the high gene expression observed when using the hydrodynamics and physical pressure-mediated methods [21,22,27]. However, there are few reports that the transcriptional process is activated by US exposure in vivo. Moreover, there is little information that the transcriptional activation followed by US exposure involves in the enhanced gene expression by in vitro and in vivo gene transfection using sonoporation method.

Our present study investigated the involvement of transcriptional processes in enhanced gene expression obtained by transfection using unmodified and Man-PEG_{2000} bubble lipoplexes with US exposure. We examined the gene transfection efficiency obtained by US-mediated gene transfection using pDNAs controlled by various transcription factors including AP-1, NFκB, cyclic adenosine 3′,5′-monophosphate response element (CRE) and serum response element (SRE), in RAW264.7 cell lines, primary mouse cultured macrophages, and mice. Then, we evaluated the gene expression and intranuclear transport of transcription factors, such as AP-1 [28] and NFκB [29,30], followed by gene transfection using unmodified and Man-PEG_{2000} bubble lipoplexes with US exposure, both in vitro and in vivo. Finally, the involvement of activated transcription on inflammatory cytokine production was also examined, since activation of specific transcriptional factors might contribute to the inflammatory responses [31,32].

2. Materials and methods

2.1. Materials

1,2-Distearoyl-*sn*-glycero-3-trimethylammoniumpropane (DSTAP), 1,2-distearoyl-*sn*-glycero-3-phosphocholine (DSPC) and 1,2-distearoyl-*sn*-glycero-3-phosphoethanolamine-N-[amino (polyethylene glycol)-2000] (NH_2-PEG_{2000}-DSPE) were purchased from Avanti Polar Lipids (Alabaster, AL, USA), Sigma-Aldrich (St. Louis, MO, USA) and NOF (Tokyo, Japan), respectively. RPMI-1640 was purchased from Nissui Pharmaceutical (Tokyo, Japan) and fetal bovine serum (FBS) was purchased from Japan Bioserum (Hiroshima, Japan). All other chemicals were of the highest purity available.

2.2. pDNA, cell lines and mice

pCMV-Luc was constructed as described previously [33]. Briefly, the HindIII/Xba I firefly luciferase cDNA fragment from pGL3-control vector (Promega, Madison, WI, USA) was sub-cloned into the polylinker of pcDNA3 vector (Invitrogen, Carlsbad, CA, USA). Pathway profiling luciferase systems (pTA/Luc, pAP-1/Luc, pNFκB/Luc, pCRE/Luc and pSRE/Luc) were purchased from Clontech Laboratories (Mountain View, CA, USA). pDNA was amplified in the *Escherichia coli* strain DH5α, isolated and purified using a QIAGEN Endofree Plasmid Giga Kit (QIAGEN, Hilden, Germany). RAW264.7 cells, from a murine macrophage-like cell line, were cultured in RPMI-1640 supplemented with 10% FBS, 100 IU/ml penicillin, 100 μg/ml streptomycin, and 2 mM L-glutamine. Cells were plated onto 24-well culture plates at a density of 5×10^4 cells/1.88 cm^2 at 37 °C in 5% CO_2, and incubated for 48 h prior to experiments. Female ICR mice (4-week-old) and female C57BL/6 mice (6-week-old) were purchased from Japan SLC (Shizuoka, Japan). All animal experiments were carried out in accordance with the Principles of Laboratory Animal Care, as adopted and propagated by the U.S. National Institutes of Health and the Kyoto University Guidelines for Animal Experiments.

2.3. Construction of Man-PEG_{2000} bubble lipoplexes

Man-PEG_{2000} bubble lipoplexes were constructed according to our previous report [17]. Briefly, DSTAP, DSPC, and NH_2-PEG_{2000}-DSPE or mannose-modified PEG_{2000}-DSPE were mixed in chloroform at a molar ratio of 7:2:1 to produce the liposomes for bubble lipoplexes. The liposome construction mixture was dried by evaporation and vacuum desiccated before the resultant lipid film was resuspended in sterile 5% dextrose. After hydration for 30 min at 65 °C, the dispersion was sonicated for 10 min in a bath sonicator and 3 min in a tip sonicator for liposome production. Liposomes were then sterilized by passage through a 0.45 μm filter (PALL, East Hills, NY, USA). Lipoplexes were prepared by gently mixing with equal volumes of pDNA and liposome solution at a charge ratio of 1.0:2.3 (−:+). Prepared lipoplexes were pressurized with perfluoropropane gas (Takachiho Chemical Industries, Tokyo, Japan) and sonicated using a bath-type sonicator (AS ONE, Osaka, Japan) for 5 min to enclose US imaging gas. Particle sizes and ζ-potentials of the liposomes/lipoplexes were determined using a Zetasizer Nano ZS instrument (Malvern Instrument, Worcestershire, UK).

2.4. Harvesting of mouse peritoneal macrophages

Mouse peritoneal macrophages were harvested and cultured as previously described [34]. Briefly, the macrophages were harvested from the peritoneal cavity of female ICR mice, before being washed and suspended in RPMI-1640 medium supplemented with 10% FBS, 100 IU/ml penicillin, 100 μg/ml streptomycin and 2 mM L-glutamine, and plated onto 24-well culture plates at a density of 2×10^5 cells/1.88 cm^2. After incubation for 2 h at 37 °C in 5% CO_2, non-adherent cells were washed off with culture medium, and the macrophages were incubated for another 72 h.

2.5. In vitro gene transfection

After RAW264.7 cells and macrophages were plated and incubated for 48 and 72 h, respectively, the culture medium was replaced with Opti-MEM I containing bubble lipoplexes (5 μg pDNA). Cells were exposed to US (frequency, 2.062 MHz; duty, 50%; burst rate, 10 Hz; intensity 4.0 W/cm^2) for 20 s using a Sonopore-4000 sonicator (NEPA GENE, Chiba, Japan) with a 6 mm diameter probe placed in each well at predetermined times after the addition of bubble lipoplexes. At 1 h after addition of bubble lipoplexes, the incubation medium was replaced with RPMI-1640 and incubated for an additional time. Subsequently, the cells were scraped from the plates and suspended in lysis buffer (0.05% Triton X-100, 2 mM EDTA, 0.1 M Tris, pH 7.8). The cell suspension was shaken, and centrifuged at 10,000×g, 4 °C for 10 min. Luciferase assay buffer (Picagene; Toyo Ink, Tokyo, Japan) was mixed with the supernatant and the luciferase activity was measured in a luminometer (Lumat LB 9507; EG&G Berthold, Bad Wildbad, Germany). Luciferase activity was normalized against the cellular protein content. Protein concentration was determined with a Protein Quantification Kit (Dojindo Molecular Technologies, Tokyo, Japan).

2.6. In vivo gene transfection

Mice were intravenously injected with 400 μl of bubble lipoplexes via the tail vein using a 26-gauge syringe needle at a dose of 50 μg pDNA. At predetermined times after the injection, US (frequency, 1.045 MHz; duty, 50%; burst rate, 10 Hz; intensity 1.0 W/cm^2; time, 2 min) was exposed transdermally to the abdominal area using a Sonopore-4000 sonicator (NEPA GENE) with a 20 mm diameter probe. At predetermined times after injection, mice were sacrificed and organs were collected for each experiment. Organs were washed twice with cold saline and homogenized with lysis buffer (0.05% Triton X-100, 2 mM EDTA, 0.1 M Tris, pH 7.8). Lysis buffer was added at a weight ratio of 5 ml/g for the liver or 4 ml/g for other organs. After 3 cycles of freezing and thawing, the homogenates were centrifuged at 10,000×g at 4 °C for 10 min. Luciferase activity of the resulting supernatant was determined by above-mentioned luciferase assay.

2.7. Quantitative reverse transcription-polymerase chain reaction (RT-PCR)

Total ribonucleic acid (RNA) was isolated from the cells and organs using a GenElute Mammalian Total RNA Miniprep Kit (Sigma-Aldrich). Reverse transcription of messenger RNA (mRNA) was carried out using PrimeScript® RT reagent Kit (Takara Bio, Shiga, Japan). The detection of complementary deoxyribonucleic acid (cDNA) (*c-fos*, *c-jun*, *p105*, *p65* and *gapdh*) was conducted using real-time PCR using SYBR® Premix Ex Taq (Takara Bio) and a Lightcycler Quick System 350S (Roche Diagnostics, Indianapolis, IN, USA). Primers for *c-fos*, *c-jun*, *p105*, *p65* and *gapdh* cDNA were synthesized by Sigma-Aldrich as follows: *c-fos*, 5′-CCA GTC AAG AGC ATC AGC AA-3′ (forward) and 5′-AAG TAG TGC AGC CCG GAG TA-3′ (reverse); *c-jun*, 5′-TCC CCT ATC GAC ATG GAG TC-3′ (forward) and 5′-TGA GTT GGC ACC CAC TGT TA-3′ (reverse); *p105*, 5′-CCT GGA TGA CTC TTG GGA AA-3′ (forward) and 5′-TCA GCC AGC TGT TTC ATG TC-3′ (reverse); *p65*, 5′-TAG CAC CTG ATG GCT GAC TG-3′ (forward) and 5′-CGT TCC ACC ACA TCT GTG TC-3′ (reverse); *gapdh*, 5′-TCT CCT GCG ACT TCA ACA-3′ (forward) and 5′-GCT GTA GCC GTA TTC ATT GT-3′ (reverse). mRNA copy number was calculated for each sample from the standard curve using the thermal-cycler software ('Arithmetic Fit Point analysis' for the Lightcycler). Results were expressed as relative copy number calculated relative to *gapdh* mRNA (*c-fos*, *c-jun*, *p105*, *p65* mRNA copy number/*gapdh* mRNA copy number).

2.8. Measurement of the level of intranuclear protein

Cells and tissues were collected at predetermined times after gene transfection, and the nuclear extract from cells and tissues was prepared using a Nuclear Extract Kit (Active Motif, Carlsbad, CA, USA). Nuclear protein was divided into aliquots and stored at −80 °C for later use. The protein concentration was measured with a Protein Quantification Kit. The amounts of p50 and p65, which are the components of NFκB in the cellular nuclear extract was measured using a NFκB (p50) Transcription Factor Kit (Thermo Fisher Scientific, Waltham, MA, USA) and a NFκB (p65) transcription Factor Assay Kit (Cayman Chemical, Ann Arbor, MI, USA), respectively, according to the manufacturer's protocols.

2.9. Measurement of inflammatory cytokines

At predetermined times after the in vitro and in vivo gene transfection, the supernatants and serum were collected and the cytokine levels (TNF-α, IFN-γ, and IL-6) were determined with a commercial enzyme-linked immunosorbent assay (ELISA) Kit (Bay Bioscience, Hyogo, Japan) according to the recommended procedures.

2.10. Statistical analysis

Results were presented as the mean ± S.D. of more than three experiments. Analysis of variance (ANOVA) was used to test the statistical significance of differences among groups. Two-group comparisons were performed by Student's *t*-test. Multiple comparisons between control and test groups were performed by Dunnett's test and multiple comparisons between all groups were performed using the Tukey–Kramer test.

3. Results

3.1. Physicochemical properties of lipoplexes and bubble lipoplexes used in this study

The physicochemical properties of lipoplexes and bubble lipoplexes constructed with various pDNAs used in all experiments were evaluated by measuring the particle sizes and ζ-potentials. Mean particle sizes and ζ-potentials of unmodified and Man-PEG_{2000} lipoplexes were approximately 137 nm and +48 mV, respectively (Supplementary Table 1). Moreover, mean particle sizes and ζ-potentials of unmodified and Man-PEG_{2000} bubble lipoplexes were approximately 550 nm and +48 mV, respectively (Supplementary Table 1). These results correspond to previous reports [17–19]; suggesting that these pDNA had no effect on the physicochemical properties of lipoplexes and bubble lipoplexes.

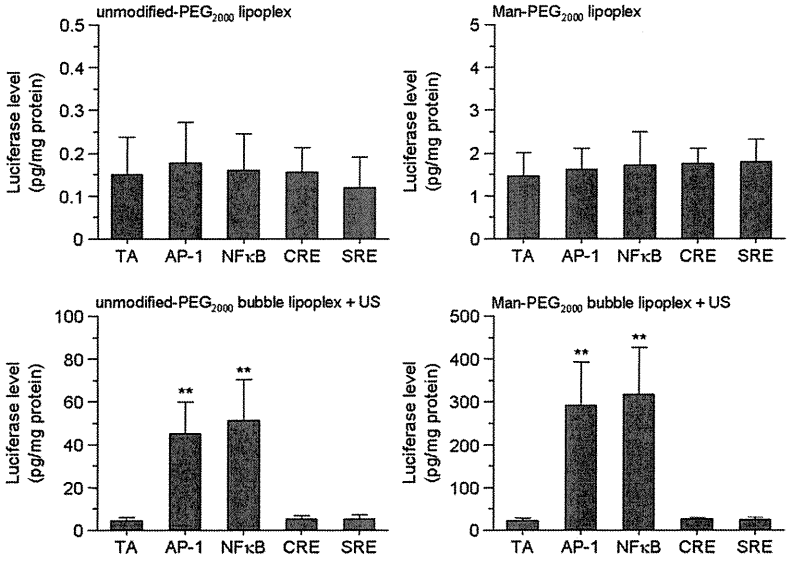

Fig. 1. The effect of transcriptional factors on gene expression obtained by unmodified and Man-PEG_{2000} bubble lipoplexes with or without US exposure in mouse cultured macrophages. Luciferase expression levels obtained by unmodified-PEG_{2000} lipoplexes, Man-PEG_{2000} lipoplexes, unmodified-PEG_{2000} bubble lipoplexes with US exposure, and Man-PEG_{2000} bubble lipoplexes with US exposure (5 μg of pDNA) at 24 h after transfection in mouse primary cultured macrophages. Lipoplexes were constructed with pDNAs controlled by various transcription factors. Each value represents the mean + S.D. ($n = 4$). Key: TA; pTA/Luc, AP-1; pAP-1/Luc, NFκB; pNFκB/Luc, CRE; pCRE/Luc, SRE; pSRE/Luc. $^{**}p<0.01$, compared with the corresponding TA group.

3.2. Involvement of transcriptional process on enhanced gene expression obtained by unmodified and Man-PEG$_{2000}$ bubble lipoplexes with US exposure in vitro

The involvement of transcription on enhanced gene expression obtained by unmodified and Man-PEG$_{2000}$ bubble lipoplexes with US exposure was investigated in mouse primary cultured macrophages. First, we examined gene expression levels using unmodified/Man-PEG$_{2000}$ lipoplexes or bubble lipoplexes constructed with luciferase expressing-pDNA controlled by various transcription factors, including AP-1, NFκB, CRE and SRE. Gene expression levels obtained by Man-PEG$_{2000}$ lipoplexes only or Man-PEG$_{2000}$ bubble lipoplexes with US exposure were higher than those by unmodified-PEG$_{2000}$ formulations (Fig. 1), since mouse cultured macrophages express the mannose receptors abundantly. Moreover, although the level of gene expression obtained by both lipoplexes was similar in all pDNAs, the level of gene expression obtained by both bubble lipoplexes and US exposure was enhanced approximately 10-fold by gene transfection using pAP-1/Luc and pNFκB/Luc, compared with that using pTA/Luc, which is a pDNA without transcription factor-binding site within the enhancer region (Fig. 1). Similar results were observed in the murine macrophage-like RAW264.7 cells (Supplementary Fig. 1).

3.3. Involvement of transcriptional process on enhanced gene expression obtained by unmodified and Man-PEG$_{2000}$ bubble lipoplexes with US exposure in mice

Next, we investigated the level of gene expression by in vivo gene transfection using unmodified/Man-PEG$_{2000}$ lipoplexes and bubble lipoplexes constructed with luciferase expressing-pDNA controlled by

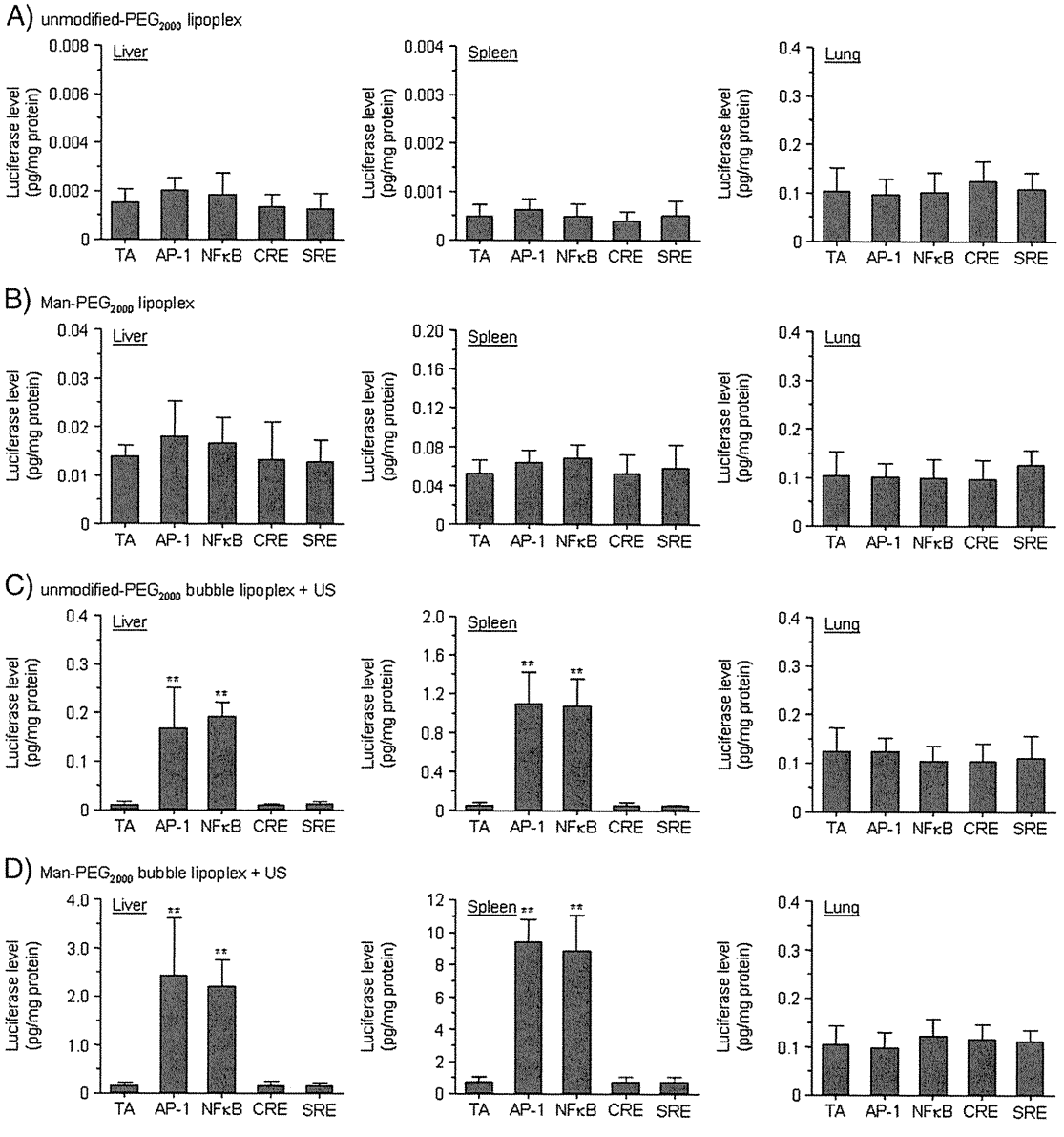

Fig. 2. The effect of transcriptional factors on gene expression obtained by unmodified and Man-PEG$_{2000}$ bubble lipoplexes with or without US exposure in vivo. Luciferase expression levels obtained by unmodified-PEG$_{2000}$ lipoplexes (A), Man-PEG$_{2000}$ lipoplexes (B), unmodified-PEG$_{2000}$ bubble lipoplexes with US exposure (C), and Man-PEG$_{2000}$ bubble lipoplexes with US exposure (D) (50 μg of pDNA) in the liver, spleen and lung at 6 h after transfection. Lipoplexes were constructed with pDNAs controlled by various types of transcriptional factors. Each value represents the mean + S.D. ($n=4$). Key: TA; pTA/Luc, AP-1; pAP-1/Luc, NFκB; pNFκB/Luc, CRE; pCRE/Luc, SRE; pSRE/Luc. $^{**}p<0.01$, compared with the corresponding TA group.

various transcription factors. Gene expression levels in the liver and spleen obtained by Man-PEG_{2000} lipoplexes only or Man-PEG_{2000} bubble lipoplexes with US exposure were higher than those by unmodified-PEG_{2000} formulations (Fig. 2), since liver and spleen are the major target organ of mannose-modified carriers. Although the level of gene expression obtained by both lipoplexes was similar in all pDNAs (Fig. 2A and B), gene expression levels in the liver and spleen obtained by both bubble lipoplexes and US exposure were enhanced approximately 10-fold by gene transfection using pAP-1/Luc and pNFκB/Luc, compared with that using pTA/Luc (Fig. 2C and D). On the other hand, enhanced gene expression followed by gene transfection using bubble lipoplexes constructed with pAP-1/Luc or pNFκB/Luc was not observed in the lung.

3.4. The effect of in vitro gene transfection using unmodified and Man-PEG_{2000} bubble lipoplexes with US exposure on AP-1 and NFκB

Following examination of the expression properties for c-fos and c-jun, which are the components of AP-1, *c-fos* and *c-jun* mRNA expression was enhanced transiently in mouse primary cultured macrophages by not only the gene transfection using bubble lipoplexes and US exposure, but also US exposure alone (Fig. 3A). Moreover, enhanced expression of *c-fos* and *c-jun* mRNA was not observed in the gene transfection using lipoplexes only (Fig. 3A). Evaluation of the expressing properties and intranuclear transporting properties of NFκB followed by gene transfection revealed that *p105* (precursor of p50) and *p65* mRNA expression in mouse primary cultured macrophages was not enhanced in all of groups, which differed from the results obtained for *c-fos* and *c-jun* mRNA (Supplementary Fig. 2). In contrast, the amount of intranuclear p50 and p65 increased transiently by not only the gene transfection using bubble lipoplexes and US exposure, but also US exposure alone (Fig. 3B). On the other hand, enhanced intranuclear transport of p50 and p65 was not observed in the gene transfection using lipoplexes only (Fig. 3B). Moreover, these transient AP-1 expression and intranuclear transport of NFκB followed by US exposure were also observed in RAW264.7 cells in this gene transfection method (Supplementary Fig. 3). These results suggest that transcription activation, such as increased AP-1 expression and enhanced intranuclear transport of NFκB, is partly involved in enhanced gene expression produced by unmodified and Man-PEG_{2000} bubble lipoplexes with US exposure.

3.5. The effect of in vivo gene transfection using unmodified and Man-PEG_{2000} bubble lipoplexes with US exposure on AP-1 and NFκB

c-fos/c-jun mRNA expression and the intranuclear amount of p50/p65 were enhanced transiently by not only the gene transfection using bubble lipoplexes and US exposure, but also US exposure alone in both the liver and spleen (Figs. 4 and 5). On the other hand, these phenomena were not observed in the lung (Figs. 4C and 5C). In addition, *c-fos* and *c-jun* mRNA expression levels in the liver and spleen followed by US exposure were dependedent on the US intensity (Supplementary Fig. 4).

3.6. The effect of in vitro and in vivo gene transfection using unmodified and Man-PEG_{2000} bubble lipoplexes and US exposure on inflammatory cytokine production

Increased AP-1 expression and intranuclear transport of NFκB followed by US exposure were demonstrated to be involved in the enhanced gene expression by unmodified and Man-PEG_{2000} bubble lipoplexes with US exposure. On the other hand, since these phenomena are potentially involved in the production of inflammatory cytokines [31,32], the production properties of inflammatory cytokines followed by gene transfection were investigated in vitro and in vivo. Although TNF-αproduction followed by gene transfection using only lipoplexes was significantly increased time-dependently in RAW264.7 cells and mouse primary cultured macrophages, only a slight increase in TNF-α production was observed followed by gene transfection using bubble lipoplexes and US exposure (Fig. 6).

While the inflammatory cytokines (TNF-α, IFN-γ, and IL-6) in the serum followed by in vivo gene transfection exhibited transient and significant increases in all of gene transfection methods (Fig. 7), the

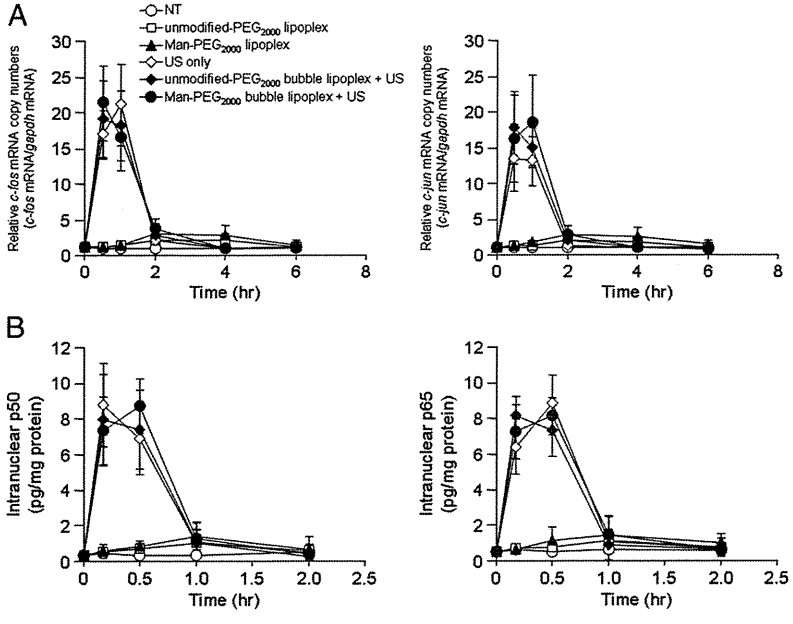

Fig. 3. Enhanced *c-fos/c-jun* mRNA expression and intranuclear transport of p105/p65 followed by gene transfection using unmodified and Man-PEG_{2000} bubble lipoplexes with or without US exposure in mouse primary cultured macrophages. Time-course of *c-fos/c-jun* mRNA expression levels (A) and intranuclear p105/p65 levels (B) followed by various transfection methods (5 μg of pCMV-Luc) in mouse primary cultured macrophages. Each value represents the mean ± S.D. ($n = 4$). $^{**}p<0.01$, compared with the corresponding non-treatment (NT) group.

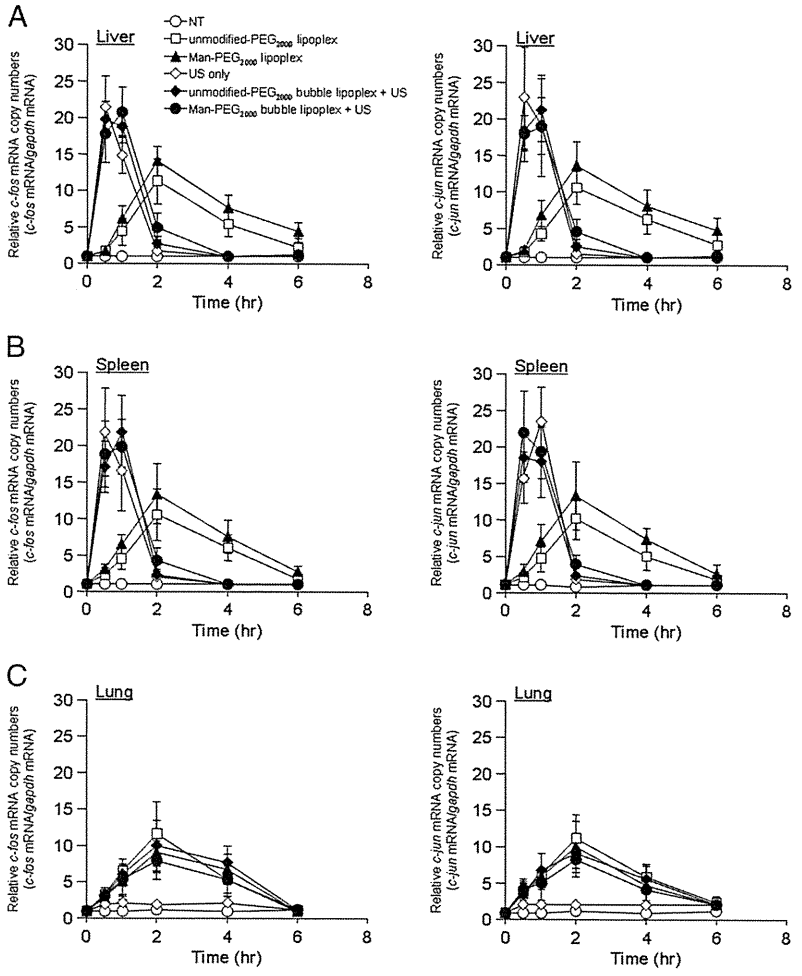

Fig. 4. Enhanced *c-fos/c-jun* mRNA expression followed by gene transfection using unmodified and Man-PEG_{2000} bubble lipoplexes with or without US exposure in vivo. Time-course of *c-fos* and *c-jun* mRNA expression levels in the liver (A), spleen (B), and lung (C) followed by various transfection methods (50 μg of pCMV-Luc) in mice. Each value represents the mean ± S.D. ($n = 4$). NT; non-treatment.

maximum amount of secreted inflammatory cytokines followed by gene transfection using bubble lipoplexes and US exposure was 3-fold lower than that using lipoplexes only. Moreover, the time-to-maximum concentration of secreted inflammatory cytokines followed by gene transfection using bubble lipoplexes and US exposure was earlier than that using only lipoplexes (Fig. 7). These results suggest that the production properties of inflammatory cytokine are different between conventional lipofection methods and US-mediated gene transfection methods, and that inflammatory cytokines have a minor effect on enhanced AP-1 expression/NFκB intranuclear transport followed by US exposure.

4. Discussion

We recently reported that large amounts of pDNA are directly transferred into the cytoplasm in the gene transfection using unmodified and Man-PEG_{2000} bubble lipoplexes with US exposure [17,19]. However, this enhanced gene expression followed by gene transfection using unmodified and Man-PEG_{2000} bubble lipoplexes with US exposure may not correspond to the increase of intracellular pDNA by targeted delivery of pDNA and intracytoplasmic transfer of pDNA; suggesting the involvement of the other factors on the enhanced gene expression in the gene transfection using both bubble lipoplexes and US exposure. It has been reported that the transcriptional process following intranuclear transport of pDNA is important factor in gene transfection efficiency [7,8]; therefore, we investigated the involvement of transcriptional processes in gene transfection using unmodified and Man-PEG_{2000} bubble lipoplexes with US exposure.

Following examination of gene expression levels using luciferase-expressing pDNAs controlled by various transcription factors, including AP-1, NFκB, CRE and SRE, we found that the level of gene expression obtained by both lipoplexes in vitro (Fig. 1 and Supplementary Fig. 1), and in mouse liver and spleen (Fig. 2A and B), was similar in all pDNAs studied. On the other hand, gene expression levels using pAP-1/Luc and pNFκB/Luc were approximately 10-fold higher than those using other pDNAs in the gene transfection using unmodified and Man-PEG_{2000} bubble lipoplexes with US exposure in vitro (Fig. 1 and Supplementary Fig. 1), and in mouse liver and spleen (Fig. 2C and D). These results strongly suggest that AP-1 and NFκB were involved in the enhanced gene expression obtained by unmodified and Man-PEG_{2000} bubble lipoplexes with US exposure. Therefore, we further investigated the AP-1/NFκB gene expression and intranuclear transport followed by this gene transfection method.

c-fos/c-jun mRNA expression (Figs. 3A and 4) and intranuclear p50/p65 levels (Figs. 3B and 5) were enhanced transiently by not only the gene transfection using both bubble lipoplexes and US exposure,

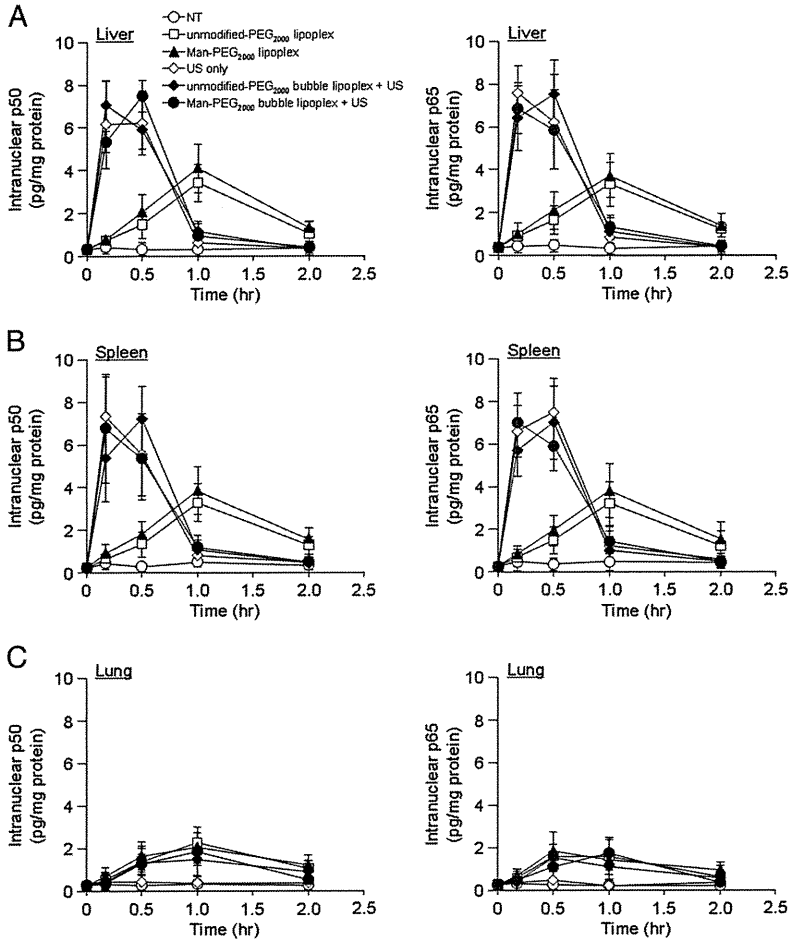

Fig. 5. Enhanced intranuclear transport of p50 and p65 followed by gene transfection using unmodified and Man-PEG_{2000} bubble lipoplexes with or without US exposure in vivo. Time-course of intranuclear p50 and p65 levels in the liver (A), spleen (B), and lung (C) followed by various transfection methods (50 μg of pCMV-Luc) in mice. Each value represents the mean ± S.D. ($n = 3$). NT; non-treatment.

but also US exposure alone in vitro, and in mouse liver and spleen. It has been reported that US exposure induced the enhanced expression of c-fos and c-jun via phosphorylation of ERK, p38 and JNK [25,26], and our results partially correspond to these reports. These observations led us to believe that the activation of AP-1 and NFκB-mediated transcriptional processes followed by US exposure is involved in the enhanced gene expression using unmodified and Man-PEG_{2000} bubble lipoplexes with US exposure.

Since the activation of transcription factors such as AP-1 [28] and NFκB [29,30] is involved in the induction of inflammatory responses [31,32], we investigated the production properties of inflammatory cytokines followed by this gene transfection method. The production levels of TNF-α, IFN-γ or IL-6 followed by gene transfection using both bubble lipoplexes and US exposure were substantially lower than that using both lipoplexes in vitro (Fig. 6) and in vivo (Fig. 7). We previously reported that the inflammatory responses were significantly suppressed in the gene transfection method using unmodified and Man-PEG_{2000} bubble lipoplexes with US exposure, because a large amount of pDNA was transferred into the cytoplasm directly through the transient pores created by the destruction of both bubble lipoplexes followed by US exposure [19], suggesting that pDNA is hardly interacted with endosomal TLR-9. On the other hand, it was reported that the phosphorylation of AP-1 and NFκB was induced via the activation of p38, ERK and JNK-mediated pathways followed by US exposure [25,26], and we showed that these AP-1 and NFκB activation was transiently in our sonoporation method and condition in this study (Figs. 3–5 and Supplementary Fig. 3). Although these activation of AP-1 and NFκB leads to the inflammatory cytokine production [31,32], the inflammatory responses induced by AP-1 and NFκB activation followed by US exposure were low under in vitro and in vivo condition (Figs. 6 and 7). We previously have reported that the activating level of transcriptional factors, such as c-fos and c-jun, in tissue pressure-mediated transfection method was approximately one-fifth, compared with that in hydrodynamics method [22]. Moreover, the production of inflammatory cytokines under in vivo condition followed by tissue pressure-mediated transfection method was much lower than those by conventional lipofection method [35]. The activating levels of transcriptional factors followed by our sonoporation method using unmodified and Man-PEG_{2000} bubble lipoplexes with US exposure were almost the same with that by tissue pressure-mediated transfection method. Therefore, the contribution of the inflammatory response induced by AP-1 and NFκB activation followed by our sonoporation method may be negligible. These results suggest that the transient expression of AP-1 and the transient intranuclear transport of NFκB followed by US exposure might be minimally involved in the inflammatory responses in the gene transfection using unmodified and Man-PEG_{2000} bubble lipoplexes with US exposure.

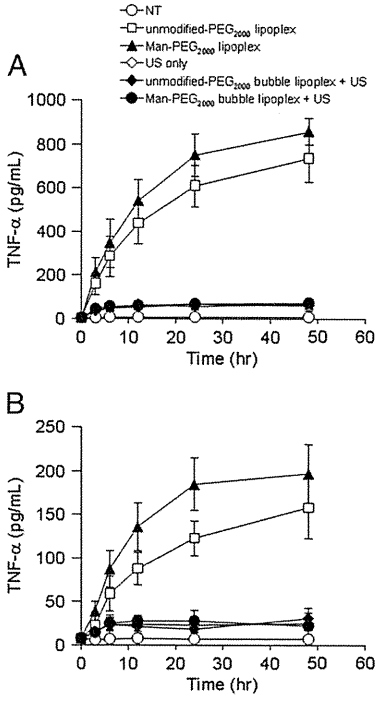

Fig. 6. Evaluation of TNF-α secretion followed by gene transfection using unmodified and Man-PEG_{2000} bubble lipoplexes with or without US exposure in vitro. TNF-α concentration in the supernatant was measured following various transfection methods (5 μg of pDNA) at predetermined times in RAW264.7 cells (A) and mouse primary cultured macrophages (B). Each value represents the mean ± S.D. ($n = 4$).

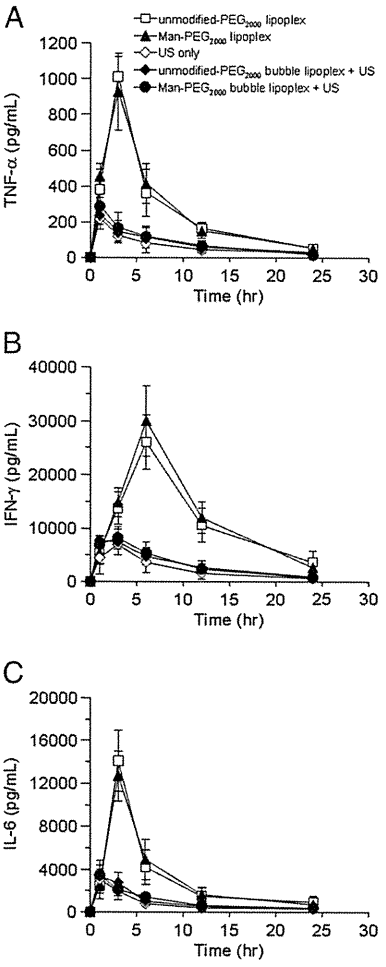

Fig. 7. Evaluation of pro-inflammatory cytokine secretion in serum followed by gene transfection using unmodified and Man-PEG_{2000} bubble lipoplexes with or without US exposure in vivo. TNF-α (A), IFN-γ (B), and IL-6 (C) concentrations in the serum were measured following various transfection methods (50 μg of pDNA) at predetermined times in mice. Each value represents the mean ± S.D. ($n = 4$).

5. Conclusion

Our results suggest that the activated AP-1 and NFκB followed by US exposure is involved in the enhanced gene expression using unmodified and Man-PEG_{2000} bubble lipoplexes with US exposure. These results suggest that enhanced gene expression in the gene transfection using our sonoporation method was obtained by applying pDNA controlled by the specific transcriptional factors. Therefore, the selection of suitable pDNA with specific promoter regions activated by US stimulation is one of the important factors for efficient gene expression in our gene transfection method. In addition, the transient expression of AP-1 and the transient intranuclear transport of NFκB followed by US exposure were not substantially involved in the inflammatory responses in this gene transfection method. These findings may help in the development of an effective gene transfection method using US-exposing system.

Acknowledgments

This work was supported in part by a Grant-in-Aid for Young Scientists (A) from the Ministry of Education, Culture, Sports, Science and Technology of Japan, and by Health and Labour Sciences Research Grants for Research on Noninvasive and Minimally Invasive Medical Devices from the Ministry of Health, Labour and Welfare of Japan, and by the Programs for Promotion of Fundamental Studies in Health Sciences of the National Institute of Biomedical Innovation (NIBIO).

Appendix A. Supplementary data

Supplementary data to this article can be found online at doi:10.1016/j.jconrel.2011.06.040.

References

[1] M. Thomas, A.M. Klibanov, Non-viral gene therapy: polycation-mediated DNA delivery, Appl. Microbiol. Biotechnol. 2003 (2003) 27–34.
[2] T. Ito, N. Iida-Tanaka, T. Niidome, T. Kawano, K. Kubo, K. Yoshikawa, T. Sato, Z. Yang, Y. Koyama, Hyaluronic acid and its derivative as a multi-functional gene expression enhancer: protection from non-specific interactions, adhesion to targeted cells, and transcriptional activation, J. Control. Release 112 (2006) 382–388.
[3] D.G. Miller, P.R. Wang, L.M. Petek, R.K. Hirata, M.S. Sands, D.W. Russell, Gene targeting in vivo by adeno-associated virus vectors, Nat. Biotechnol. 24 (2006) 1022–1026.
[4] K. Itaka, K. Yamauchi, A. Harada, K. Nakamura, H. Kawaguchi, K. Kataoka, Polyion complex micelles from plasmid DNA and poly(ethylene glycol)-poly(L-lysine) block copolymer as serum-tolerable polyplex system: physicochemical properties of micelles relevant to gene transfection efficiency, Biomaterials 24 (2003) 4495–4506.
[5] A. Kim, E.H. Lee, S.H. Choi, C.K. Kim, In vitro and in vivo transfection efficiency of a novel ultradeformable cationic liposome, Biomaterials 25 (2004) 305–313.
[6] S.M. Kwon, H.Y. Nam, T. Nam, K. Park, S. Lee, K. Kim, I.C. Kwon, J. Kim, D. Kang, J.H. Park, S.Y. Jeong, In vivo time-dependent gene expression of cationic lipid-based emulsion as a stable and biocompatible non-viral gene carrier, J. Control. Release 128 (2008) 89–97.
[7] S. Hama, H. Akita, R. Ito, H. Mizuguchi, T. Hayakawa, H. Harashima, Quantitative comparison of intracellular trafficking and nuclear transcription between adenoviral and lipoplex systems, Mol. Ther. 13 (2006) 786–794.
[8] S. Hama, H. Akita, S. Iida, H. Mizuguchi, H. Harashima, Quantitative and mechanism-based investigation of post-nuclear delivery events between adenovirus and lipoplex, Nucleic Acids Res. 35 (2007) 1533–1543.

[9] H. Potter, L. Weir, P. Leder, Enhancer-dependent expression of human kappa immunoglobulin genes introduced into mouse pre-B lymphocytes by electroporation, Proc. Natl. Acad. Sci. U.S.A. 81 (1984) 7161–7165.
[10] F. Liu, Y. Song, D. Liu, Hydrodynamics-based transfection in animals by systemic administration of plasmid DNA, Gene Ther. 6 (1999) 1258–1266.
[11] Y. He, A.A. Pimenov, J.V. Nayak, J. Plowey, L.D. Falo Jr., L. Huang, Intravenous injection of naked DNA encoding secreted flt3 ligand dramatically increases the number of dendritic cells and natural killer cells in vivo, Hum. Gene Ther. 11 (2000) 547–554.
[12] F. Liu, L. Huang, Noninvasive gene delivery to the liver by mechanical massage, Hepatology 35 (2002) 1314–1319.
[13] K. Anwer, G. Kao, B. Proctor, I. Anscombe, V. Florack, R. Earls, E. Wilson, T. McCreery, E. Unger, A. Rolland, S.M. Sullivan, Ultrasound enhancement of cationic lipid-mediated gene transfer to primary tumors following systemic administration, Gene Ther. 7 (2000) 1833–1839.
[14] G. Zhang, X. Gao, Y.K. Song, R. Vollmer, D.B. Stolz, J.Z. Gasiorowski, D.A. Dean, D. Liu, Hydroporation as the mechanism of hydrodynamic delivery, Gene Ther. 11 (2004) 675–682.
[15] Y. Negishi, Y. Endo, T. Fukuyama, R. Suzuki, T. Takizawa, D. Omata, K. Maruyama, Y. Aramaki, Delivery of siRNA into the cytoplasm by liposomal bubbles and ultrasound, J. Control. Release 132 (2008) 124–130.
[16] I. Lentacker, N. Wang, R.E. Vandenbroucke, J. Demeester, S.C. De Smedt, N.N. Sanders, Ultrasound exposure of lipoplex loaded microbubbles facilitates direct cytoplasmic entry of the lipoplexes, Mol. Pharm. 6 (2009) 457–467.
[17] K. Un, S. Kawakami, R. Suzuki, K. Maruyama, F. Yamashita, M. Hashida, Development of an ultrasound-responsive and mannose-modified gene carrier for DNA vaccine therapy, Biomaterials 31 (2010) 7813–7826.
[18] K. Un, S. Kawakami, R. Suzuki, K. Maruyama, F. Yamashita, M. Hashida, Suppression of melanoma growth and metastasis by DNA vaccination using an ultrasound-responsive and mannose-modified gene carrier, Mol. Pharm. 8 (2011) 543–554.
[19] K. Un, S. Kawakami, M. Yoshida, Y. Higuchi, R. Suzuki, K. Maruyama, F. Yamashita, M. Hashida, The elucidation of gene transferring mechanism by ultrasound-responsive unmodified and mannose-modified lipoplexes, Biomaterials 32 (2011) 4659–4669.
[20] T. Pazmany, S.P. Murphy, S.O. Gollnick, S.P. Brooks, T.B. Tomasi, Activation of multiple transcription factors and fos and jun gene family expression in cells exposed to a single electric pulse, Exp. Cell Res. 221 (1995) 103–110.
[21] M. Nishikawa, A. Nakayama, Y. Takahashi, Y. Fukuhara, Y. Takakura, Reactivation of silenced transgene expression in mouse liver by rapid, large-volume injection of isotonic solution, Hum. Gene Ther. 19 (2008) 1009–1020.
[22] H. Mukai, S. Kawakami, H. Takahashi, K. Satake, F. Yamashita, M. Hashida, Key physiological phenomena governing transgene expression based on tissue pressure-mediated transfection in mice, Biol. Pharm. Bull. 33 (2010) 1627–1632.
[23] T. Tanos, M.J. Marinissen, F.C. Leskow, D. Hochbaum, H. Martinetto, J.S. Gutkind, O.A. Coso, Phosphorylation of c-Fos by members of the p38 MAPK family. Role in the AP-1 response to UV light, J. Biol. Chem. 280 (2005) 18842–18852.
[24] S. Ramanan, M. Kooshki, W. Zhao, F.C. Hsu, M.E. Robbins, PPARalpha ligands inhibit radiation-induced microglial inflammatory responses by negatively regulating NF-kappaB and AP-1 pathways, Free Radic. Biol. Med. 45 (2008) 1695–1704.
[25] Y.C. Chiu, T.H. Huang, W.M. Fu, R.S. Yang, C.H. Tang, Ultrasound stimulates MMP-13 expression through p38 and JNK pathway in osteoblasts, J. Cell. Physiol. 215 (2008) 356–365.
[26] S. Zhou, M.G. Bachem, T. Seufferlein, Y. Li, H.J. Gross, A. Schmelz, Low intensity pulsed ultrasound accelerates macrophage phagocytosis by a pathway that requires actin polymerization, Rho, and Src/MAPKs activity, Cell. Signal. 20 (2008) 695–704.
[27] H. Ochiai, M. Fujimuro, H. Yokosawa, H. Harashima, H. Kamiya, Transient activation of transgene expression by hydrodynamics-based injection may cause rapid decrease in plasmid DNA expression, Gene Ther. 14 (2007) 1152–1159.
[28] R. Eferl, E.F. Wagner, AP-1: a double-edged sword in tumorigenesis, Nat. Rev. Cancer 3 (2003) 859–868.
[29] N.D. Perkins, Integrating cell-signalling pathways with NF-kappaB and IKK function, Nat. Rev. Mol. Cell Biol. 8 (2007) 49–62.
[30] S.G. Pereira, F. Oakley, Nuclear factor-kappaB1: regulation and function, Int. J. Biochem. Cell Biol. 40 (2008) 1425–1430.
[31] A. Cloutier, T. Ear, O. Borissevitch, P. Larivée, P.P. McDonald, Inflammatory cytokine expression is independent of the c-Jun N-terminal kinase/AP-1 signaling cascade in human neutrophils, J. Immunol. 171 (2003) 3751–3761.
[32] A.M. Elsharkawy, D.A. Mann, Nuclear factor-kappaB and the hepatic inflammation-fibrosis-cancer axis, Hepatology 46 (2007) 590–597.
[33] T. Takagi, M. Hashiguchi, R.I. Mahato, H. Tokuda, Y. Takakura, M. Hashida, Involvement of specific mechanism in plasmid DNA uptake by mouse peritoneal macrophages, Biochem. Biophys. Res. Commun. 245 (1998) 729–733.
[34] K. Un, S. Kawakami, R. Suzuki, K. Maruyama, F. Yamashita, M. Hashida, Enhanced transfection efficiency into macrophages and dendritic cells by a combination method using mannosylated lipoplexes and bubble liposomes with ultrasound exposure, Hum. Gene Ther. 21 (2010) 65–74.
[35] H. Mukai, S. Kawakami, Y. Kamiya, F. Ma, H. Takahashi, K. Satake, K. Terao, H. Kotera, F. Yamashita, M. Hashida, Pressure-mediated transfection of murine spleen and liver, Hum. Gene Ther. 20 (2009) 1157–1167.

G Model
IJP-12173; No. of Pages 9
ARTICLE IN PRESS

International Journal of Pharmaceutics xxx (2011) xxx–xxx

Contents lists available at SciVerse ScienceDirect

International Journal of Pharmaceutics

journal homepage: www.elsevier.com/locate/ijpharm

A facile preparation method of a PFC-containing nano-sized emulsion for theranostics of solid tumors

Kouichi Shiraishi [a], Reiko Endoh [a], Hiroshi Furuhata [a], Masamichi Nishihara [b], Ryo Suzuki [c], Kazuo Maruyama [c], Yusuke Oda [c], Jun-ichiro Jo [d], Yasuhiko Tabata [d], Jun Yamamoto [e], Masayuki Yokoyama [a,*]

[a] Medical Engineering Laboratory, Research Center for Medical Science, The Jikei University School of Medicine, 3-25-8, Nishi-shinbashi, Minato-ku, Tokyo 105-8461, Japan
[b] International Institute for Carbon-Neutral Energy Research (I²CNER), Kyushu University, 744 Motooka, Nishi-ku, Fukuoka 819-0395, Japan
[c] Department of Biopharmaceutics, School of Pharmaceutical Sciences, Teikyo University, 1091-1 Suwarashi, Midori-ku, Sagamihara, Kanagawa 252-5195, Japan
[d] Department of Biomaterials, Institute for Frontier Medical Sciences, Kyoto University, 53 Kawara-cho Shogoin, Sakyo-ku, Kyoto 606-8507, Japan
[e] Division of Physics and Astronomy, Graduate School of Science, Kyoto University, Kitashirakawa Oiwake-cho, Sakyo-ku, Kyoto 606-8502, Japan

ARTICLE INFO

Article history:
Received 14 June 2011
Received in revised form 27 August 2011
Accepted 2 October 2011
Available online xxx

Keywords:
Theranostics
Tumor targeting
Ultrasound
Perfluorocarbon
Emulsion

ABSTRACT

Theranostics means a therapy conducted in a diagnosis-guided manner. For theranostics of solid tumors by means of ultrasound, we designed a nano-sized emulsion containing perfluoropentane (PFC5). This emulsion can be delivered into tumor tissues through the tumor vasculatures owing to its nano-size, and the emulsion is transformed into a micron-sized bubble upon sonication through phase transition of PFC5. The micron-sized bubbles can more efficiently absorb ultrasonic energy for better diagnostic images and can exhibit more efficient ultrasound-driven therapeutic effects than nano-sized bubbles. For more efficient tumor delivery, smaller size is preferable, yet the preparation of a smaller emulsion is technically more difficult. In this paper, we used a bath-type sonicator to successfully obtain small PFC5-containing emulsions in a diameter of ca. 200 nm. Additionally, we prepared these small emulsions at 40 °C, which is above the boiling temperature of PFC5. Accordingly, we succeeded in obtaining very small nano-emulsions for theranostics through a very facile method.

1. Introduction

'Theranostics', 'theranosis', or 'theragnosis' is a newly created term in the fields of imaging diagnosis and drug delivery systems. As a word, 'theranostics' (Chen, 2011; Lammers et al., 2010, 2011; MacKay and Li, 2010) is a combination of therapy and diagnosis, and is defined as therapy conducted in a diagnosis-guided manner. A typical example of theranostics is found in a carrier system containing both a contrast agent for diagnosis and a drug for therapy. Theranostics has been studied with various types of drug carriers including liposomes (Kamaly and Miller, 2010), small molecules (Kalber et al., 2011), nano-particles (Jeong et al., 2011; Kim et al., 2010), emulsions (Gianella et al., 2011), synthetic polymers (Bryson et al., 2009), polymeric micelles (Blanco et al., 2009; Kaida et al., 2010; Min et al., 2010; Nakamura et al., 2006; Shiraishi et al., 2009, 2010), and other nano-sized carrier systems (Ai, 2011; Moon et al., 2011; Pan et al., 2008; Sanson et al., 2011). Ultrasound is considered to be a preferable modality for theranostics because ultrasound has been well studied and developed for image diagnoses and local therapies such as ultrasound lithotresis and hyperthermia.

For theranostics of solid tumors, micron-sized bubbles (microbubbles) (Hernot and Klibanov, 2008; Schutt et al., 2003; Unger et al., 2004) have been actively studied because the bubbles provide strong contrasts in ultrasonic images, and because cavitation of microbubbles (Grishenkov et al., 2009) induced by ultrasound can effectively damage cells. Cells can be damaged by both jet-stream and heat that are generated in the bubbles' cavitation. In the design of microbubbles for tumor applications, the size of the microbubbles is a very important factor. Larger microbubbles can produce stronger ultrasound image contrasts. In contrast, smaller bubbles are preferred for efficient delivery into tumor tissues because the size of the trans-vascular passage from the bloodstream into the tumor interstitial space is of a diameter smaller than 1 μm. It is believed that the maximum diameter for efficient translocation into tumor tissues is 200–400 nm (Ishida et al., 1999; Litzinger et al., 1994; Nagayasu et al., 1996; Yuan et al., 1995). (In this diameter range, bubbles must be called nano-bubbles.) This is an essential dilemma concerning the size of bubbles used for

Abbreviations: PFC, perfluorocarbon; PFC5, perfluoropentane; PFC6, perfluorohexane; DBU, 1,8-diazabicyclo[5.4.0]undec-7-ene; PEG-P(Asp(C7F9)x), poly(ethylene glycol)-b-poly(4,4,5,5,6,6,7,7,7-nonafluoroheptyl aspartate) block copolymer.

* Corresponding author. Tel.: +81 3 3433 1111x2336; fax: +81 3 3459 6005.
E-mail address: masajun2093ryo@jikei.ac.jp (M. Yokoyama).

0378-5173/$ – see front matter © 2011 Elsevier B.V. All rights reserved.
doi:10.1016/j.ijpharm.2011.10.006

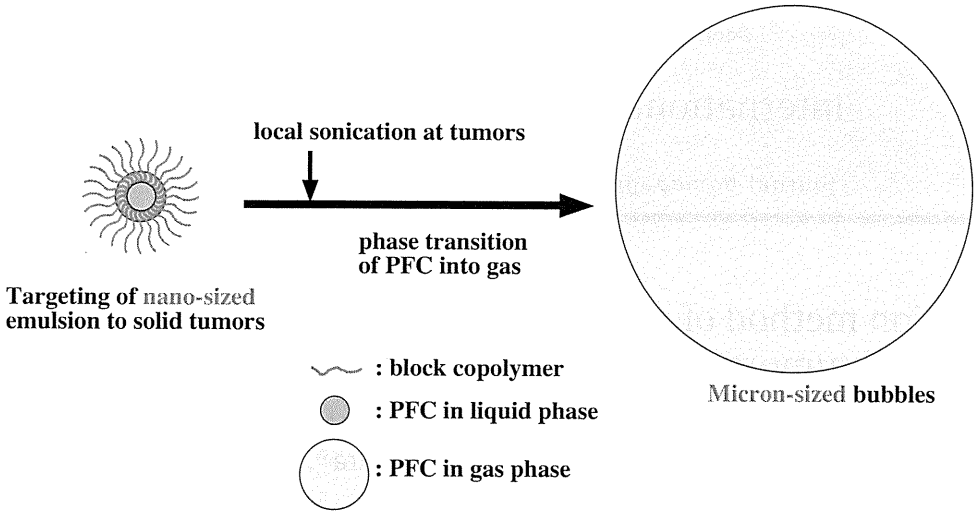

Fig. 1. Concept of phase-transition type nano-emulsion.

tumor theranostics. In order to resolve this dilemma, Kawabata et al. (Asami et al., 2009, 2010; Kawabata et al., 2005, 2010a,b) and Rapoport et al. (Mohan and Rapoport, 2010; Rapoport et al., 2007, 2009a, 2009b, 2010a,b, in press) examined nano-emulsions incorporating a specific kind of perfluorocarbon, as illustrated in Fig. 1. A boiling temperature of this perfluorocarbon (perfluoropentane, PFC5) is 29 °C, which is lower than normal human body temperature, but the integrity of these nano-emulsions is maintained owing to interfacial excessive pressure called Laplace pressure (Rapoport et al., 2009a). Upon ultrasound irradiation, the integrity of these nano-emulsions is broken, and this liquid perfluorocarbon exhibits a phase-transition into gas. Accordingly, the nano-emulsions change into microbubbles. Efficient delivery into tumor tissues is attained with the nano-emulsions, and then local sonication at the tumor tissues generates the microbubbles from the nano-emulsions, resulting in high imaging and therapeutic efficiencies. This phase-transition type nano-emulsion may be an ideal system for the theranostics of solid tumors.

Generally, preparations of smaller emulsions in a nano-meter range are more difficult because a higher power input is required in the emulsion preparations. (Tadros et al., 2004) Previously, we had prepared perfluorocarbon-containing emulsions by means of vigorous mechanical stirring with a magnetic stirrer and obtained emulsions of ca. 600 nm in diameter (Nishihara et al., 2009). In this paper, we have tried to obtain much smaller emulsions by means of ultrasound irradiation as well as high-pressure emulsification. Another important parameter for preparations of the phase-transition type nano-emulsion is temperature. A boiling temperature (29 °C) of perfluoropentane (PFC5) is close to the room temperature; therefore, preparations must be carried out at a low temperature and in a small scale for evasion of evaporation of PFC5 because heat generated in emulsification or sonication processes must be efficiently removed for the evasion. We want to find a facile preparation method that can be carried out at either room or a higher temperature, and that can be easily scaled up because the heat removal is a much less serious concern than the conventional method. Rapoport et al. (Rapoport et al., 2010b) reported preparations of nano-bubbles by means of ultrasound irradiation (with a probe type sonicator at 20 kHz) in ice-cold water. They obtained nano-emulsions of ca. 600 nm in diameter.

In this paper, we have tried to obtain very small nano-emulsions containing PFC5 by using an inexpensive bath-type sonicator (usually used as an ultrasonic cleaner) at room temperature or higher. For this emulsion preparation, we synthesized fluorinated block copolymers and optimized their compositions.

2. Materials and methods

2.1. Materials

We purchased perfluoropentane (PFC5) and perfluorohexane (PFC6) from Stream Chemicals (Newburyport, MA, USA) and Alfa Aesar (Ward Hill, MA, USA), respectively, and used them as received. We purchased 4,4,5,5,6,6,7,7,7-nonafluoroheptyl iodide from Sigma–Aldrich (Tokyo branch, Japan) and used it as received. We purchased reagent-grade solvents, dehydrated *N*,*N*-dimethylformamide (DMF), dimethyl sulfoxide (DMSO), and diethyl ether from Wako Chemicals (Tokyo, Japan), and used them as received. Poly(L-lactic acid)-grafted gelatin was prepared through a coupling reaction between a primary amine group of gelatin and a terminal hydroxyl group of the poly(L-lactic acid) by the use of disuccimidyl carbonate according to a published synthetic procedure. (Tanigo et al., 2010) Poly(ethylene glycol)-block-poly(L-lactic acid) block copolymer (PEG-b-PLA) was purchased from Sigma–Aldrich (Tokyo branch, Japan). The average molecular weights of the PEG block and the PLA block were 750 and 1,000, respectively.

2.2. Block copolymer synthesis

Poly(ethylene glycol)-*b*-poly(4,4,5,5,6,6,7,7,7-nonafluoroheptyl aspartate) block copolymers (PEG-P(Asp(C7F9)*x*)) were prepared by means of esterification of the aspartic units of poly(ethylene glycol)-b-poly(aspartic acid) block copolymer (PEG-P(Asp)) by the use of an iodinated compound, as shown in Fig. 2. PEG-P(Asp) was synthesized according to our previous paper (Yamamoto et al., 2007). A value *x* in the PEG-P(Asp(C7F9)*x*) formula denotes mol.% of the esterified units. This esterification reaction was carried out with a corresponding iodinated compound in the presence of a super base according to a previously reported procedure (Opanasopit et al., 2004; Yokoyama et al., 2004; Yamamoto et al., 2007) with a slight modification.

The starting material was poly(ethylene glycol)-b-poly(aspartic acid) block copolymer (PEG-P(Asp)). The average molecular weight of PEG was 5200 (n = 119 in Fig. 2), and the average number of Asp units per one chain was 26.0. The aspartate amide bond can be either α or β, and our group previously had reported that a ratio of α:β was 1:3 (=*a*:*b* in Fig. 2) (Yokoyama et al., 2004). PEG-P(Asp) (2.001 g, containing 6.33×10^{-3} mol Asp residue) was dissolved in 20 mL of DMF. To this mixture, was added both 4.904 g of 4,4,5,5,6,6,7,7,7-nonafluorohepty iodide (which is

Please cite this article in press as: Shiraishi, K., et al., A facile preparation method of a PFC-containing nano-sized emulsion for theranostics of solid tumors. Int J Pharmaceut (2011), doi:10.1016/j.ijpharm.2011.10.006

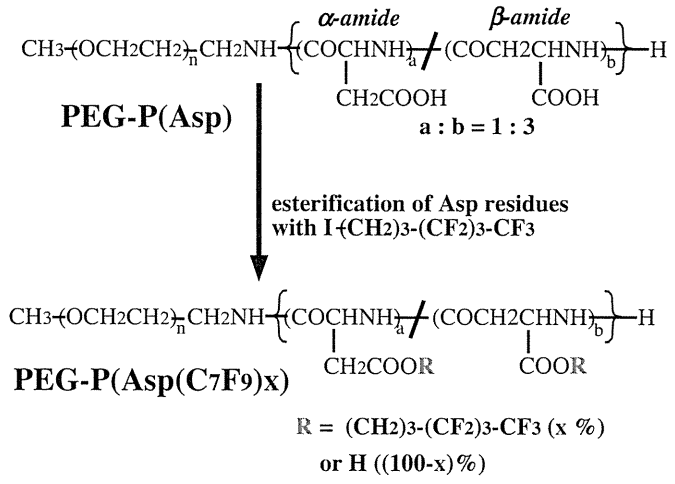

Fig. 2. Synthesis of the fluorocarbon-containing block copolymer PEG-P(Asp(C7F9)*x*).

2.00 mol. equivalents to the Asp residue, I-(CH2)3-(CF2)3-CF3 in Fig. 2) and 0.972 g of 1,8-diazabicyclo[5.4.0]undec-7-ene (DBU, which is 1.01 mol. equivalents to the Asp residue). DBU is a very strong base, and can induce ionization in a carboxyl group of the aspartic acid residue in an organic solvent, DMF. The reaction mixture was heated at 50 °C for 16 h. An ester formed at the Asp residue through a nucleophilic substitution reaction of the ionized carboxyl group with I-(CH2)3-(CF2)3-CF3. After this 16-h reaction, the reaction mixture was poured into 200 mL of ice-cold diethyl ether for precipitation of the polymer. The precipitated polymer was filtered and washed with diethyl ether. The obtained polymer was dissolved in 20 mL of DMSO, to which was added 2.11 mL of 6 N hydrochloric acid. This acid works for removal of DBU from polymers. This polymer solution was dialyzed with a Spectra/Por 6 dialysis membrane (molecular weight cut-off is 1000) against DMSO for 2 days and against milliQ water for an additional 2 days, followed by freeze-drying. Yield was 2.436 g. To determine the contents of the fluorinated ester group of the polymer, we used ^{1}H NMR spectroscopy in DMSO-d_6 containing 3 v/v% trifluoroacetic acid. For this determination, we identified a peak area ratio between the methylene protons ($-COOCH_2\underline{CH_2}CH_2CF_2CF_2CF_2CF_3$) at 1.8 ppm of the ester group and the methylene protons ($-OCH_2\underline{CH_2}-$) at 3.6 ppm of the PEG block. The esterification percentage (x in Fig. 2) was revealed to be 59%. The other compositions of block copolymers were synthesized according to the same method with various molar ratios of I-(CH2)3-(CF2)3-CF3 and DBU with respect to the aspartic acid residue. Table 1 lists all the compositions of the synthesized block copolymers.

Table 1
Compositions of PEG-P(Asp(C7F9)*x*).

Code	M.W. of PEG	Asp unit number (n)	Esterification degree (x%)
F-6%	5200	22.1	5.9
F-15%	5200	23.3	14.6
F-39%	5200	22.1	38.5
F-59%	5200	26.0	58.5
F-67%	5200	22.1	67.0

2.3. Preparation of PFC-containing nano-emulsions

We examined preparations of PFC5-containing nano-emulsions according to two methods using a high-pressure emulsifier and a bath-type sonicator.

2.3.1. Preparation with a high-pressure emulsifier

We dissolved PEG-P(Asp(C7F9)15) block copolymer by stirring it in distilled water at a concentration of 4.0 wt. % of the solution, and added perfluoropentane (PFC5) and perfluorohexane (PFC6) at each 1.25 vol.% of the solution. We vigorously stirred the solution with a homogenizer Polytron (Kinematica AG, Tokyo, Japan) at 25,000 rpm for 10 s. Then, we conducted emulsification using a high-pressure emulsifier EmulsiFlex-C5 CSC (AVESTIN, Inc., Ottawa, Ontario, Canada) at 4 °C for 6 min at ca. 50 MPa. We collected a white emulsion, and filtered it with a Sartorius Minisart (R) filter (1.2 μm pore, Sartorius AG, Göttingen, Germany).

2.3.2. Preparation with a bath-type sonicator

We dissolved PEG-P(Asp(C7F9)*x*) block copolymers in MilliQ water at a concentration of 1.0 to 4.0 wt.% of water. In case of a high ester content such as x = 59, we heated (up to ca. 40 °C) and sonicated the solutions until we obtained a transparent polymer solution. The polymer solution was transferred to a 1.5-mL glass vial that was sealed with a Teflon–silicon rubber cap (Chromacol auto-sampler vial 2-SV for HPLC; GL Science, Inc., Tokyo, Japan), and was cooled on ice. Then, we added perfluoropentane (PFC5) and perfluorohexane (PFC6) at 0.5–4.0 vol.% of water. We confirmed PFCs' position at the bottom of the solution. (Sometimes PFCs, whose densities are much greater than water's, did not go into the aqueous solution. Therefore, we shook the vial vigorously to allow PFC droplets to sink to the bottom by force of gravity.) Then, we sealed the vial with a cap, and applied sonication for 3 min with a bath-type sonicator Branson model 1510 (oscillating frequency at 42 kHz, max. power intensity: 90 W, Danbury, CT, USA). The temperature of the bath was kept constant with degassed cold and hot water. In all the sonication procedures, we had a constant water level in a sonicator bath and a fixed position of the vial in order to obtain sonication conditions that were as identical to one another as possible. Finally, we collected a supernatant by leaving unincorporated PFC droplets at the bottom.

Table 2
Effects of polymer composition and sample volume on PFC5 incorporation behaviors.

Run	Polymer	Sample volume (μL)	PFC5 concentration (vol.%)[a]	Cumulant average diameter (nm)[a]
1	F-6%	300	0.840 ± 0.097	261.2 ± 3.4
2	F-15%	300	0.948 ± 0.131	232.4 ± 14.5
3	F-39%	300	0.625 ± 0.074	198.4 ± 33.3
4	F-59%	300	0.669[b]	133.9[b]
5	F-67%	300	0.682 ± 0.060	222.8 ± 37.9
6	F-59%	300	0.682 ± 0.074	205.5 ± 15.8
7	F-59%	300	0.634 ± 0.361	173.5 ± 24.5
8	F-59%	700	1.110[b]	231.8[b]
9	F-59%	1200	1.792[b]	280.6[b]

[a] Average ± standard deviation (n = 3) except runs 4, 8, and 9.
[b] Average of two preparations.

Please cite this article in press as: Shiraishi, K., et al., A facile preparation method of a PFC-containing nano-sized emulsion for theranostics of solid tumors. Int J Pharmaceut (2011), doi:10.1016/j.ijpharm.2011.10.006